



This discussion paper is/has been under review for the journal Geoscientific Model Development (GMD). Please refer to the corresponding final paper in GMD if available.

# Improved simulation of fire-vegetation interactions in the Land surface Processes and eXchanges dynamic global vegetation model (LPX-Mv1)

D. I. Kelley<sup>1</sup>, S. P. Harrison<sup>1,2</sup>, and I. C. Prentice<sup>1,3</sup>

<sup>1</sup>Department of Biological Sciences, Macquarie University, North Ryde, NSW 2109, Australia

<sup>2</sup>Geography & Environmental Sciences, School of Archaeology, Geography and Environmental Sciences (SAGES), University of Reading, Whiteknights, Reading, RG6 6AB, UK

<sup>3</sup>AXA Chair of Biosphere and Climate Impacts, Grantham Institute for Climate Change and Department of Life Sciences, Imperial College, Silwood Park Campus, Ascot SL5 7PY, UK

Received: 30 October 2013 – Accepted: 26 November 2013 – Published: 23 January 2014

Correspondence to: D. I. Kelley (douglas.kelley@students.mq.edu.au)

Published by Copernicus Publications on behalf of the European Geosciences Union.

Title Page

Abstract

Introduction

Conclusions

References

Tables

Figures

◀

▶

◀

▶

Back

Close

Full Screen / Esc

Printer-friendly Version

Interactive Discussion



## Abstract

The Land surface Processes and eXchanges (LPX) model is a fire-enabled dynamic global vegetation model that performs well globally but has problems representing fire regimes and vegetative mix in savannas. Here we focus on improving the fire module.

- 5 To improve the representation of ignitions, we introduced a treatment of lightning that allows the fraction of ground strikes to vary spatially and seasonally, realistically partitions strike distribution between wet and dry days, and varies the number of dry-days with strikes. Fuel availability and moisture content were improved by implementing decomposition rates specific to individual plant functional types and litter classes, and
- 10 litter drying rates driven by atmospheric water content. To improve water extraction by grasses, we use realistic plant-specific treatments of deep roots. To improve fire responses, we introduced adaptive bark thickness and post-fire resprouting for tropical and temperate broadleaf trees. All improvements are based on extensive analyses of relevant observational data sets. We test model performance for Australia, first evaluating parameterisations separately and then measuring overall behaviour against standard benchmarks. Changes to the lightning parameterisation produce a more realistic simulation of fires in southeastern and central Australia. Implementation of PFT-specific
- 15 decomposition rates enhances performance in central Australia. Changes in fuel drying improve fire in northern Australia, while changes in rooting depth produce a more realistic simulation of fuel availability and structure in central and northern Australia.
- 20 The introduction of adaptive bark thickness and resprouting produces more realistic fire regimes in savannas, including simulating biomass recovery rates consistent with observations. The new model (LPX-Mv1) improves Australian vegetation composition by 33 % and burnt area by 19 % compared to LPX.

## Parameterisation of fire in LPX1 vegetation model

D. I. Kelley et al.

[Title Page](#)

[Abstract](#)

[Introduction](#)

[Conclusions](#)

[References](#)

[Tables](#)

[Figures](#)

◀

▶

[Back](#)

[Close](#)

[Full Screen / Esc](#)

[Printer-friendly Version](#)

[Interactive Discussion](#)



# 1 Introduction

The Land surface Processes and eXchanges (LPX) dynamic global vegetation model (DGVM) incorporates fire through a coupled fire module (Prentice et al., 2011) as fire is a major agent in vegetation disturbance regimes (Bond and Van Wilgen, 1996) and contributes to changes in interannual atmospheric carbon fluxes (Prentice et al., 2011; van der Werf et al., 2008). LPX realistically simulates fire and vegetation cover globally but performs relatively poorly in grassland and savanna ecosystems (Kelley et al., 2013) – areas where fire is particularly important for maintaining vegetation diversity and ecosystem structure (e.g. Williams et al., 2002; Lehmann et al., 2008; Biganzoli et al., 2009). Specifically:

- LPX produces sharp boundaries between areas of high burning and no burning in tropical and temperate regions. These sharp fire boundaries produce sharp boundaries between grasslands and forests. The unrealistically high fire-induced tree mortality prevents the development of transitions via more open forests and woodlands.
- LPX simulates too little fire in areas of high but seasonal rainfall because fuel takes an unrealistically long time to dry, and because LPX fails to produce open woody vegetation in these areas.
- In arid areas, where fire is limited by fuel availability, LPX simulates too much Net Primary Production (NPP) resulting in unrealistically high fuel loads and generating more fire than observed.

To address these shortcomings in the version of LPX running at Macquarie University (here designated LPX-M), we re-parameterised lightning ignitions, fuel moisture, fuel decomposition, plant adaptations to arid conditions via rooting depth, and woody plant resistance to fire through bark thickness. In each case, the new parameterisation was developed based on extensive data analysis. We tested each parameterisation separately, and then all parametrisations combined, using a comprehensive benchmarking



system (Kelley et al., 2013) which assesses model performance against observations of key vegetation and fire processes. We then included a new treatment of woody plant recovery after fire through resprouting – a behavioural trait that increases post-fire competitiveness compared to non-resprouters in fire-prone areas (Clarke et al., 2013)

5 – and tested the impact of introducing this new component on model performance.

## 2 LPX model description

LPX is a Plant Functional Type (PFT) based model. Nine PFTs are distinguished by a combination of life form (tree, grass) and leaf type (broad, needle), phenology (evergreen, deciduous) and climate range (tropical, temperate, boreal) for trees and photosynthetic pathway ( $C_3$ ,  $C_4$ ) for grasses. PFTs are represented by a set of parameters. Each PFT that occurs within a gridcell is represented by an “average” plant, and ecosystem-level behaviour is calculated by multiplying the simulated properties of this average plant by the simulated number of individuals in the PFT in that gridcell. PFT-specific properties (e.g. establishment, mortality and growth) are updated annually, but water and carbon-exchange processes are simulated on shorter timesteps.

15 LPX incorporates a process-based fire scheme (Fig. 1) run on a daily timestep (Prentice et al., 2011). Ignition rates are derived from a monthly lightning climatology, interpolated to the daily timestep. The number of lightning strikes that reach the ground (cloud-to-ground: CG) is specified as 20 % of the total number of strikes (Thonicke et al., 2010). The CG lightning is split into dry ( $CG_{dry}$ ) and wet strikes based on the fraction of wetdays in the month ( $P_{wet}$ ):

$$CG_{dry} = CG \cdot (1 - P_{wet})^\beta \quad (1)$$

where  $\beta$  is a parameter tuned to 0.00001. “Wet” lightning is not considered to be an ignition source (Prentice et al., 2011). Lightning is finally scaled down by 85 % to allow for discontinuous current strikes. Numerical precision limits of the compiled code means the function described by Eq. (1) effectively removes all strikes in months with

[Title Page](#)

[Abstract](#)

[Introduction](#)

[Conclusions](#)

[References](#)

[Tables](#)

[Figures](#)

◀

▶

[Back](#)

[Close](#)

[Full Screen / Esc](#)

[Printer-friendly Version](#)

[Interactive Discussion](#)



more than two wet days in LPX. Monthly “dry” lightning is distributed evenly across all dry days.

Fuel loads are generated from litter production and decay using the vegetation dynamics algorithms in LPJ (Sitch et al., 2003). LPX does not simulate competition between C<sub>3</sub> and C<sub>4</sub> grasses explicitly; in gridcells where C<sub>3</sub> and C<sub>4</sub> grasses co-exist, the total NPP is estimated as the potential NPP of each grass type in the absence of the other type and this produces erroneously high NPP. This problem can be corrected by scaling the fractional projective cover (FPC) and Leaf Area Index (LAI) of each grass PFT by the ratio of total simulated grass leaf mass of both PFTs to the leaf mass expected if only one grass PFT was present (B. Stocker, personal communication, 2012)

Fuel decomposition rate ( $k$ ) depends on temperature and moisture, and is the same for all PFTs and fuel structure types:

$$k = k_{10} \cdot g(T) \cdot f(w) \quad (2)$$

where  $k_{10}$  is a decomposition rate at a reference temperature of 10 °C, set to 35 % each year;  $g(T)$  describes the response to monthly mean soil temperature ( $T_{\text{soil, m}}$ ) described by Lloyd and Taylor (1994):

$$g(T) = \begin{cases} e^{308.56 \cdot \left( \frac{1}{56.02} - \frac{1}{T_{\text{soil, m}} + 46.02} \right)}, & \text{if } T_{\text{soil, m}} \geq -40 \\ 0, & \text{otherwise} \end{cases} \quad (3)$$

and  $f(w)$  is the moisture response to the top layer soil water content ( $w$ ) described by Foley (1995)

$$f(w) = 0.25 + 0.75 \cdot w \quad (4)$$

where  $w$  is in fractional water content.

The litter is allocated to four fuel categories based on litter size as described by Thonicke et al. (2010):

[Title Page](#)

[Abstract](#)

[Introduction](#)

[Conclusions](#)

[References](#)

[Tables](#)

[Figures](#)

◀

▶

◀

▶

[Back](#)

[Close](#)

[Full Screen / Esc](#)

[Printer-friendly Version](#)

[Interactive Discussion](#)



- *1 h fuel* – which represents leaves and small twigs, is the leaf and herb mass plus 4.5 % of the litter that comes from tree heart- and sapwood;
- *10 h fuel* – representing small branches, is 7.5 % of the litter from heart- and sapwood
- *100 h fuel* – large branches, is 21 % of the litter that comes from heart- and sapwood
- *1000 h fuel* – boles and trunks, is the remaining 67 % of the litter that comes from heart- and sapwood.

The hour designation represents the decay rate of fuel moisture, and is equal to the amount of time for the moisture of the fuel to become  $(1 - 1/\exp)$  63 % closer to the moisture of its surroundings (Albini, 1976; Anderson et al., 1982).

In LPX, litter drying rate is described by the cumulative Nesterov Fire Danger Index (NI: Nesterov, 1949) as described by Running (1987), and a fuel-specific drying rate parameter ( $\alpha_{xhr}$ : Venevsky et al., 2002) which was tuned to provide the best results against fire observations (Thonicke et al., 2010). NI is cumulated for each consecutive day with rainfall  $\leq 3$  mm, and is calculated using maximum daily temperature ( $T_{\max}$ ) and an approximation of dew point:

$$T_{\text{dew}} = T_{\min} - 4 \quad (5)$$

where  $T_{\min}$  is the daily minimum temperature and both  $T_{\min}$  and  $T_{\max}$  are in °C.

Daily precipitation is simulated based on monthly precipitation and fractional wet days using a simple weather generator (Gerten et al., 2004), and the diurnal temperature range is calculated from daily maximum and minimum temperature interpolated from monthly data.

Fire spread, intensity and residence time are based on weather conditions and fuel moisture, and calculated using the Rothermel equations (Rothermel, 1972). Fire intensity and residence time influence fire mortality via crown scorching and cambial damage.

## Parameterisation of fire in LPX1 vegetation model

D. I. Kelley et al.

[Title Page](#)

[Abstract](#)

[Introduction](#)

[Conclusions](#)

[References](#)

[Tables](#)

[Figures](#)

◀

▶

◀

▶

[Back](#)

[Close](#)

[Full Screen / Esc](#)

[Printer-friendly Version](#)

[Interactive Discussion](#)



## Parameterisation of fire in LPX1 vegetation model

D. I. Kelley et al.

[Title Page](#)

[Abstract](#)

[Introduction](#)

[Conclusions](#)

[References](#)

[Tables](#)

[Figures](#)

[◀](#)

[▶](#)

[◀](#)

[▶](#)

[Back](#)

[Close](#)

[Full Screen / Esc](#)

[Printer-friendly Version](#)

[Interactive Discussion](#)



The amount of cambial damage is determined by fire intensity and residence time in relation to bark thickness, with thicker bark offering protection for longer fire residence times. Bark thickness (BT) is calculated as a linear function of tree diameter at breast height (DBH), with specific slope and intercept values for each PFT:

$$5 \quad BT = a + b \cdot DBH \quad (6)$$

The values of  $a$  and  $b$  can be found in Thonicke et al. (2010).

The probability of mortality from cambial damage ( $P_m$ ) is calculated from the fire residence time ( $\tau_l$ ) and a critical time till cambial damage ( $\tau_c$ ) based on bark thickness:

$$10 \quad P_m(\tau) = \begin{cases} 0, & \text{if } \frac{\tau_l}{\tau_c} \leq 0.22 \\ 0.563 \cdot \frac{\tau_l}{\tau_c} - 0.125, & \text{if } 0.22 \leq \frac{\tau_l}{\tau_c} \leq 2 \\ 1, & \text{if } \frac{\tau_l}{\tau_c} \geq 2 \end{cases} \quad (7)$$

and

$$5 \quad \tau_c = 2.9 \cdot BT^2 \quad (8)$$

where  $\tau$  is the ratio  $\tau_l/\tau_c$ . Both  $\tau_l$  and  $\tau_c$  are in minutes and BT is in cm.

LPX uses a two-layer soil model. The water content of the upper (50 cm) layer is the difference between through-fall (precipitation – interception) and evapotranspiration (ET), runoff and percolation to the lower soil layer. Water content in the lower 1 m layer is the difference between percolation from the upper layer, transpiration from deep roots and runoff (Gerten et al., 2004). The upper soil layer responds more rapidly to changes in inputs, whereas the water content of the lower soil layer is generally more stable. The fraction of roots in each soil layer is a PFT-specific parameter.

### 3 Changes to the LPX-M fire module

Improvements to the LPX-M fire module focussed on re-parameterisation of lightning ignitions, fuel drying rate, fuel decomposition rate, rooting depth, and the introduction of adaptive bark thickness and of resprouting.

#### 5 3.1 Lightning ignitions

Regional studies have shown that the CG proportion of total lightning strikes varies between 0.1–50 % of total strikes. This variability has been related to latitude (Price and Rind, 1993; Pierce, 1970; Prentice and Mackerras, 1977), storm size (Kuleshov and Jayaratne, 2004), total flash count (Baldocchi et al., 2000), and topography (Baldocchi et al., 2000; de Souza et al., 2009). We compared the remotely-sensed flash counts of total flash counts (i.e. Inter-Cloud, or IC, plus CG) from the Lightning Imaging Sensor (LIS – Christian et al., 1999; Christian, 1999, <http://grip.nsstc.nasa.gov/>) with the National Lightning Detection Network Database (NLDN) records of lightning ground-strikes (CG) for the contiguous United States (available at <http://thunderstorm.vaisala.com/>; Cummins and Murphy, 2009), for each month in 2005 at the 0.5° resolution of LPX. These analyses were confined to south of 35° N, a limitation imposed by satellite coverage of the total strikes (Christian et al., 1999).

LIS observed each cell for roughly 90 s each overpass with 11–21 overpasses each month depending on latitude (Christian et al., 1999), and therefore only represents a sample of the total lightning. Overpasses for each 0.5 ° cell have a time stamp for the start and end of each overpass, along with detection efficiency and total observation time, which allows for observational blackouts. We scaled the flash count from each overpass for detection efficiency and the ratio of observed to total overpass time. These scaled flash counts were summed for each month, to give monthly recorded total (IC + CG) lightning, RL.

NLDN registered each ground lightning strike separately with a time stamp accurate to 1/1000th of a second, which allowed us to calculate the number of ground-registered

GMDD

7, 931–1000, 2014

Parameterisation of  
fire in LPX1  
vegetation model

D. I. Kelley et al.

Title Page

Abstract

Introduction

Conclusions

References

Tables

Figures

◀

▶

Back

Close

Full Screen / Esc

Printer-friendly Version

Interactive Discussion



NLDN strikes for each LIS overpass. This number of ground strikes was then scaled for a universal detection efficiency of 90 % (Baldocchi et al., 2000; Cummins and Murphy, 2009), and summed up for the month, to give monthly recorded CG strikes (RG). The CG fraction was taken as RG/RL. Total flash count ( $L$ ) was calculated by scaling the

total ground registered lightning for each month by the CG fraction. The relationship between fractional CG and total lightning was determined using non-linear least squares regression, testing for both power and exponential functions. The best (Fig. 2a) was given by:

$$10 \quad CG = L \cdot \min(1, 0.0001267 \cdot L^{-0.4180}) \quad (9)$$

where  $L$  is in flash/m<sup>2</sup>/month. We also tested topography and topographic complexity, calculated from topographic data from WORLDCLIM (Hijmans et al., 2005). These variables were not significantly related to the observed CG fraction, and so we have not included them as predictors in the new parameterisation.

15 We examined the relationship between CG strikes and the daily distribution of precipitation using the CPC US Unified Precipitation data (Higgins and Centre, 2000; Higgins et al., 1996) provided by the NOAA/OAR/ESRL PSD, Boulder, Colorado, USA (<http://www.esrl.noaa.gov/psd/>). Days are classified as dry if there was zero precipitation. We used data for every month of 2005, this time covering the whole of the contiguous United States. We used Generalised Linear Modelling (GLM; Hastie and Pregibon, 20 1992) to compare CG<sub>dry</sub> to  $P_{wet}$  and monthly precipitation from CPC and CRU TS3.1 (Harris et al., 2013), as well as temperature from CRU TS3.1 (Harris et al., 2013).  $P_{wet}$  from both CPC and CRU were the best and only significant predictors. Using CPC for consistency, the best relationship for CG<sub>dry</sub> (Fig. 2b) was:

$$25 \quad CG_{dry} = 0.85033 \cdot CG \cdot e^{-2.835 \cdot P_{wet}} \quad (10)$$

We determined a new parameter for the fraction of dry days with lightning strikes (“dry storm days”) by comparing the fraction of dry days in CPC when lightning occurred

( $P_{\text{dry, lightn}}$ ) with  $\text{CG}_{\text{dry}}$  calculated in Eq. (10) (Fig. 2c). The analysis was performed using the same spatial domain as the analysis of  $\text{CG}_{\text{dry}}$ . The best relationship with the least squared residuals (Fig. 2c) was:

$$P_{\text{dry lightn}} = 1 - \frac{1}{1.099 \cdot (\text{CG}_{\text{dry}} + 1)^{94.678.69}} \quad (11)$$

5

The results of these analyses were used in the new parameterisation of lightning in LPX-Mv1. IC lightning was removed by applying Eq. (9), where  $L$  is taken from the monthly lightning climatology inputs. Wet lightning was removed from the remaining CG strikes by applying Eq. (10). The remaining  $\text{CG}_{\text{dry}}$  was distributed evenly onto the number of dry days defined by Eq. (11). The dry lightning days were selected randomly from the days without precipitation as determined by the weather generator (Gerten et al., 2004). Discontinuous current lightning was removed at the same constant rate as in LPX because there are no data sets that would allow analyses on which to base a re-parameterisation.

15

Pfeiffer and Kaplan (2013) have argued that inter-annual variability in lightning is important, especially in high latitude regions with relatively few fires, and have introduced this in a version of LPX (LPX-SPITFIREv2) based on a scaling with convective available potential energy (CAPE). This idea was adopted from Peterson et al. (2010) who demonstrated that the probability of lightning occurring on a dry day varies inter-annually with CAPE. However, LPX-SPITFIREv2 does not contain a treatment of dry lightning nor “storm days”, so the approach taken there is parallel to ours. Murray et al. (2012) have shown that interannual variability in total flash count (i.e standard deviation of IC + CG) is < 10 % in tropical and temperate regions. This, and the fact that the LIS data set only covers a period of 10 yr and it is not obvious how to extrapolate lightning under a changing climate, mean that we have retained the use of a lightning climatology for total lightning in LPX-Mv1, but with seasonally and inter-annually varying treatments of dry lightning and dry storm days.

25

---

## Parameterisation of fire in LPX1 vegetation model

D. I. Kelley et al.

---

<a href="#">Title Page</a>	
<a href="#">Abstract</a>	<a href="#">Introduction</a>
<a href="#">Conclusions</a>	<a href="#">References</a>
<a href="#">Tables</a>	<a href="#">Figures</a>
<a href="#">◀◀</a>	<a href="#">▶▶</a>
<a href="#">◀</a>	<a href="#">▶</a>
<a href="#">Back</a>	<a href="#">Close</a>
<a href="#">Full Screen / Esc</a>	
<a href="#">Printer-friendly Version</a>	
<a href="#">Interactive Discussion</a>	



### 3.2 Fuel drying

The formulation of fuel drying in LPX results in drying times that are too slow in most tropical and temperate regions. Under stable and dry weather conditions with a  $T_{\max}$  of 30 °C and  $T_{\text{dew}}$  of 0 °C, for example, 1 h fuel in LPX would take 25 h to lose 63 % of its moisture, 10 h fuel would take roughly 20 days, 100 h fuel takes 2 months, and 1000 h fuel takes 3 yr. The approximation of  $T_{\text{dew}}$  used in LPX has been shown to be too high in arid and semi-arid areas, and during dry periods in seasonal climates (Friend, 1998; Running, 1987), which also contributes to slower-than-expected drying. Additionally, given that the moisture content is calculated cumulatively, a sequence of days with < 3 mm of rain could result in complete drying of fuel, no matter what the moisture content of the air.

In order to improve this formulation, we replace the description of fuel moisture content in LPX with one based on the moisture content of the air. As fuel types are distinguished by the time it takes for fuel to come into equilibrium with the surroundings, this new formulation is consistent with the definition of fuel types. Fuel moisture decays towards an “equilibrium moisture content” ( $m_{\text{eq}}$ ) at a rate that matches the definition of the fuel class (i.e. 1 h fuel takes 1/24th of a day to become 63 % closer to  $m_{\text{eq}}$ ):

$$m_{x,d} = \frac{m_{\text{eq}}}{100} + \left( m_{x,d-1} - \frac{m_{\text{eq}}}{100} \right) \cdot e^{-24/x} \quad (12)$$

where  $m_{x,d}$  is the daily moisture content of fuel size  $x$  hours with a moisture decay rate of  $24/x$ ; and  $m_{x,d-1}$  is the moisture content on the previous day.

There are several choices of fuel equilibrium models that could be used for  $m_{\text{eq}}$ , with variation in the magnitude of the  $m_{\text{eq}}$  response to  $H_R$ , particularly at extremes (i.e.  $H_R \rightarrow 0, 100\%$ ), and the potential for opposite responses to temperature depending on weather conditions (Sharples et al., 2009; Viney, 1991). Viney (1991) attributed this variation to the choice of fuel type for which each model was calibrated. We chose the model described by Van Wagner and Pickett (1985) for  $m_{\text{eq}}$  as it has been calibrated

[Title Page](#)[Abstract](#)[Introduction](#)[Conclusions](#)[References](#)[Tables](#)[Figures](#)[◀](#)[▶](#)[Back](#)[Close](#)[Full Screen / Esc](#)[Printer-friendly Version](#)[Interactive Discussion](#)

[Title Page](#)[Abstract](#)[Introduction](#)[Conclusions](#)[References](#)[Tables](#)[Figures](#)[◀](#)[▶](#)[◀](#)[▶](#)[Back](#)[Close](#)[Full Screen / Esc](#)[Printer-friendly Version](#)[Interactive Discussion](#)

against multiple fuel types (Van Wagner, 1972) and is designed to be more accurate at both high and low  $H_R$  (Sharples et al., 2009; Viney, 1991):

$$m_{\text{eq}} = \begin{cases} m_{\text{eq},1} + m_{\text{eq},2} + m_{\text{eq},3}, & \text{if } \text{Pr}_d \leq 3 \text{ mm} \\ 100, & \text{otherwise} \end{cases} \quad (13)$$

5 where

$$m_{\text{eq},1} = 0.942 \cdot (H_R^{0.679}) \quad (14)$$

$$m_{\text{eq},2} = 0.000499 \cdot e^{0.1 \cdot H_R} \quad (15)$$

$$m_{\text{eq},3} = 0.18 \cdot (21.1 - T_{\text{max}}) \cdot (1 - e^{-0.115 \cdot H_R}) \quad (16)$$

10  $H_R$  is calculated using the August–Roche–Magnus approximation (Lawrence, 2005), which has been shown to be accurate for  $T_{\text{dew}}$  of between 0 and 50 °C and  $T_{\text{max}}$  between 0 and 60 °C (Lawrence, 2005):

$$H_R = 100 \cdot \frac{e^{17.271 \cdot T_{\text{dew}} / (237.7 + T_{\text{dew}})}}{e^{17.271 \cdot T_{\text{max}} / (237.7 + T_{\text{max}})}} \quad (17)$$

15 We use a new formulation for  $T_{\text{dew}}$  derived from information from 20 weather stations across the United States (Kimball et al., 1997):

$$T_{\text{dew},k} = T_{\text{min},k} \cdot (-0.127 + 1.121 \cdot W_{\text{EF}} + 0.0006 \cdot \Delta T) \quad (18)$$

20 where  $T_{\text{dew},k}$  is the daily dew point temperature in Kelvin;  $\Delta T$  is the difference between daily  $T_{\text{max}}$  and  $T_{\text{min}}$ , and  $W_{\text{EF}}$  is given by:

$$W_{\text{EF}} = (1.003 - 1.444 \cdot \text{EF} + 12.312 \cdot \text{EF}^2 - 32.766 \cdot \text{EF}^3) \quad (19)$$

and EF is the ratio of daily potential evapotranspiration ( $\text{PET}_d$ ) – calculated as described in Gerten et al. (2004) – and annual precipitation ( $\text{Pr}_a$ ):

$$25 \text{ EF} = \text{PET}_d / \text{Pr}_a \quad (20)$$

Kimball et al. (1997) showed that this approximation of  $T_{\text{dew}}$  improved the correlation with  $T_{\text{dew}}$  measurements by 20 % when tested against 32 independent weather stations, with  $T_{\text{dew}}$  showing differences up to 20 °C in semi-arid and arid climates.

### 3.3 Fuel decomposition

- 5 Fuel decomposition rates vary with the size and type of material (Cornwell et al., 2008, 2009; Weedon et al., 2009; Chave et al., 2009). Brovkin et al. (2012) analysed decomposition rates derived from the TRY database (Kattge et al., 2011) and showed that there was an order of magnitude difference in the decomposition rates of wood and leaf/grass litter. Thus, grass decomposes at an average rate of 94 % per year, while  
10 wood decomposes at a rate of 5.7 % per year. The rate of both leaf and wood decomposition varies between PFTs to a lesser extent than between wood and grass, although the variation is still significant (Brovkin et al., 2012), with leaf decomposition ranging between 76 % and 120 %, and wood between 3.9 % and 10.4 % per year (Table 1). Brovkin et al. (2012) also showed that the decomposition rates of woody material  
15 are not moisture dependent.

We have implemented the PFT-specific relationships found by Brovkin et al. (2012), for woody ( $k_{10,\text{wood}}$  for 10–1000 h fuel – see Table 1) and leaf ( $k_{10,\text{leaf}}$  for 1 h fuel – see Table 1) litters. We use a relationship between decomposition and temperature for woody fuel that removes the soil moisture dependence in LPX:

$$20 \quad k_{\text{wood}} = k_{10,\text{wood}} \cdot Q_{10}^{(T_{m,\text{soil}} - 10)/10} \quad (21)$$

$Q_{10}$  is the PFT-specific temperature response of wood decomposition described in Table 1 and  $k_{10,\text{wood}}$  is the decomposition rate at a reference temperature of 10 °C. Leaf decomposition still follows Eq. (2).

[Title Page](#)

[Abstract](#)

[Introduction](#)

[Conclusions](#)

[References](#)

[Tables](#)

[Figures](#)

◀

▶

◀

▶

[Back](#)

[Close](#)

[Full Screen / Esc](#)

[Printer-friendly Version](#)

[Interactive Discussion](#)



### 3.4 Rooting depth

There are inconsistencies in the values used in LPX-M for the fraction of deep roots specified for each PFT. For example, the fraction of deep roots specified for C<sub>4</sub> grasses (20%) is greater than the fraction specified for tropical broadleaf evergreen trees (15%), even though trees have deeper roots than grasses (Schenk and Jackson, 2005). Additionally, benchmarking against arid grassland and desert litter production shows that simulated fine litter production is roughly 250% of observations. Having a high proportion of deep roots allows plants to survive more arid conditions, thanks to a more stable water supply in deep soil.

We re-examined the PFT-specific values assigned to rooting fraction using site-based data for the cumulative rooting fraction depth from Schenk and Jackson (2002a, b, 2005). In the original publications, life form, leaf type, leaf phenology and the cause of leaf fall (i.e. cold or drought) were recorded for each site. This allowed us to classify sites into LPX PFTs as shown in Table 2. The original data source does not distinguish 10 different types of grassland. We therefore separated these sites into warm (C<sub>4</sub> dominated) and cool (C<sub>3</sub> dominated) grasslands depending on their location and climate. Sites were allocated to warm grassland if they occurred in locations where the mean 15 temperature of the coldest month (MTCO) was > 15.5 °C and to cool grasslands where MTCO was ≤ 15.5 °C as per Harrison et al. (2010). MTCO for each site was based on 20 average conditions for 1970–2000 derived from the CRU TS3.1 data set (Harris et al., 2013).

The rooting-depth dataset gives the cumulative fraction depth of 50 % ( $D_{50}$ ) and 95 % ( $D_{95}$ ) of the roots at a site. These were used to calculate the cumulative root fraction at 50 cm (i.e the fraction in the upper soil layer):

$$25 \quad R_{50\text{cm}} = 1/(1 + (0.5/D_{50}^c)) \quad (22)$$

where

[Title Page](#)[Abstract](#)[Introduction](#)[Conclusions](#)[References](#)[Tables](#)[Figures](#)[◀](#)[▶](#)[◀](#)[▶](#)[Back](#)[Close](#)[Full Screen / Esc](#)[Printer-friendly Version](#)[Interactive Discussion](#)

$$c = \frac{\log 0.5/0.95}{\log D_{95}/D_{50}} \quad (23)$$

We derived Eqs. (22) and (23) by re-arranging Eq. (1) in Schenk and Jackson (2002b).

The PFT-specific (Fig. 3) fraction of deep roots ( $DR_{pft}$ ) is then implemented as:

<sup>5</sup>  $DR_{pft} = 1 - \text{mean}(R_{50\text{cm},pft}) \quad (24)$

See Table 1 for new parameter values.

### 3.5 Bark thickness

There is considerable variability in bark thickness between different tree species

<sup>10</sup> (Halliwell and Apps, 1997; Fyllas and Patino, 2009; Paine et al., 2010), such that it is unrealistic to prescribe a single constant value for the relationship between bark thickness and stem diameter within a PFT. Furthermore, bark thickness within related species appears to vary as a function of environmental conditions, and most particularly with fire frequency (Brando et al., 2012; Climent et al., 2004; Cochrane, 2003; <sup>15</sup> Lawes et al., 2011a). Thus, at an ecosystem-level, bark thickness is an adaptive trait.

We assess the relationship between bark thickness and stem diameter based on 13297 measurements from 1364 species (see Supplement for information on the studies these were obtained from). The species were classified into PFTs based on their leaf type, phenology and climate range (Table A1); in cases where this was not provided by the original data contributors, we used information from trait databases, floras and the literature (e.g Kauffman, 1991; Greene et al., 1999; Bellingham and Sparrow, <sup>20</sup> 2000; Williams, 2000; Bond and Midgley, 2001; Del Tredici, 2001; Pausas et al., 2004; Paula et al., 2009; Lunt et al., 2011). The climate range was based on the overall range of the species, not derived from the climate of the sites.

For each PFT, we calculated the best fit and the 5–95 % range (Koenker, 2013, Fig. 4) using the simple linear relationship:

$$BT_i = \text{par}_i \cdot DBH \quad (25)$$

- 5 where  $i$  is either: best fit (mid); 5 % (lower); 95 % (upper) ranges. Values for  $\text{par}_i$  are given in Table 1.

We define a probability distribution of bark thicknesses for each PFT, using a triangular relationship defined by the 5 and 95 % limits of the observations (Fig. 4):

$$T(BT) = \begin{cases} 0, & \text{if } BT \leq BT_{\text{lower}} \\ T_1(BT), & \text{if } BT_{\text{lower}} \leq BT \leq BT_{\text{mid}} \\ T_2(BT), & \text{if } BT_{\text{mid}} \leq BT \leq BT_{\text{upper}} \\ 0, & \text{if } BT \geq BT_{\text{upper}} \end{cases} \quad (26)$$

10

where  $BT_{\text{lower}}/BT_{\text{upper}}/BT_{\text{mid}}$  is the upper/lower/mid range of BT for a given DBH, calculated using Eq. (25), with  $\text{par}_i$  values in Table 1; and

$$T_1(BT) = \frac{2 \cdot (BT - BT_{\text{lower}})}{(BT_{\text{upper}} - BT_{\text{lower}}) \cdot (BT_{\text{mid}} - BT_{\text{lower}})} \quad (27)$$

$$T_2(BT) = \frac{2 \cdot (BT_{\text{upper}} - BT)}{(BT_{\text{upper}} - BT_{\text{lower}}) \cdot (BT_{\text{lower}} - BT_{\text{mid}})} \quad (28)$$

15

The distribution is initialized using  $\text{par}_i$  values in Table 1.  $\text{par}_{\text{lower}}$  and  $\text{par}_{\text{upper}}$  remain unchanged from the initial value (Table 1).  $\text{par}_{\text{mid}}$  changes each day there is a fire event based on the bark thickness of surviving plants and annually from establishment, based on the combined bark thickness of new and existing plants (Fig. 5).

The average bark thickness of trees surviving fire is dependent on the current state of  $T(BT)$  and  $P_m$  given in Eq. (7), and is calculated by solving the following integrals:

$$BT_{\text{mean}} = \frac{N_* \cdot \int_{BT_{\text{lower}}}^{BT_{\text{upper}}} BT \cdot (1 - P_m(\tau)) \cdot T(BT) dB\tau}{N} \quad (29)$$

- 5 where  $N_*$  is the number of individuals before the fire event and  $N$  the number of individuals that survive the fire, given by:

$$N = N_* \cdot \int_{BT_{\text{lower}}}^{BT_{\text{upper}}} (1 - P_m(\tau)) \cdot T(BT) dB\tau \quad (30)$$

where  $\tau$  is the ratio  $\tau_l/\tau_c$ .

- 10 A new mid point of the distribution,  $BT_{\text{mid}}$ , is calculated from  $BT_{\text{mean}}$ :

$$BT_{\text{mid}} = 3 \cdot BT_{\text{mean}} - BT_{\text{lower}} - BT_{\text{upper}} \quad (31)$$

The updated  $par_{\text{mid}}$  value is calculated from the fractional distance between  $BT_{\text{mid}}$  before the fire event ( $BT_{\text{mid},0}^*$ ), and  $BT_{\text{upper}}$ :

$$15 par_{\text{mid}} = par_{\text{mid}}^* + BT_{\text{mid,frac}} \cdot (p_{\text{upper}} - p_{\text{mid}}^*) \quad (32)$$

where  $p_{\text{mid}}^*$  was  $p_{\text{mid}}$  before the fire event and

$$BT_{\text{mid,frac}} = \frac{BT_{\text{mid}} - BT_{\text{mid},0}^*}{BT_{\text{upper}} - BT_{\text{mid},0}^*} \quad (33)$$

<a href="#">Title Page</a>	<a href="#">Abstract</a>	<a href="#">Introduction</a>
<a href="#">Conclusions</a>	<a href="#">References</a>	
<a href="#">Tables</a>	<a href="#">Figures</a>	
<a href="#">◀◀</a>	<a href="#">▶▶</a>	
<a href="#">◀</a>	<a href="#">▶</a>	
<a href="#">Back</a>	<a href="#">Close</a>	
<a href="#">Full Screen / Esc</a>		
<a href="#">Printer-friendly Version</a>		
<a href="#">Interactive Discussion</a>		



Newly-established plants have a bark thickness distribution ( $E(BT)$ ) described by Eq. (26) based on the initial  $p_{mid0}$  given in Table 1. Post-establishment  $BT_{mean}$  is calculated as the average of pre-establishment  $T(BT)$  and  $E(BT)$ , weighted by the number of newly established ( $m$ ) and old individuals ( $n$ ):

$$5 \quad BT_{mean} = \frac{\int_{BT_{lower}}^{BT_{upper}} BT \cdot (n \cdot T(BT) + m \cdot E(BT)) dB T}{n + m} \quad (34)$$

The new  $p_{mid}$  is calculated again using Eqs. (31) and (32). In cases where no trees survive fire,  $T(BT)$  is set to its initial value when the PFT re-establishes.

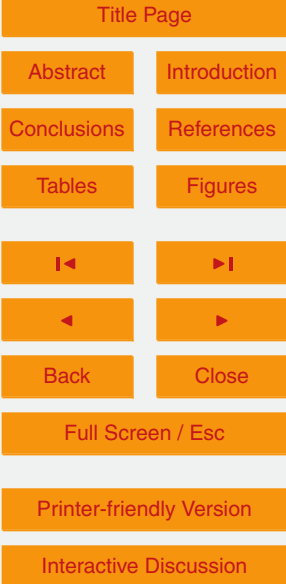
### 3.6 Resprouting

- 10 Many species have the ability to resprout from below-ground or above-ground meristems after fire (Clarke et al., 2013). Resprouting ensures rapid recovery of leaf mass, and thus conveys a competitive advantage over non-resprouting species which have to regenerate from seed. Post-fire recovery in ecosystems that include resprouting trees is fast, with ca 50 % of leaf mass being recovered within a year and full recovery within  
15 ca 5–7 yr (Viedma et al., 1997; Calvo et al., 2003; Casady, 2008; Casady et al., 2009; Gouveia et al., 2010; van Leeuwen et al., 2010; Gharun et al., 2013, see Fig. 7 and Table 5).

However, species that resprout from aerial tissue (apical or epicormic resprouters in the terminology of Clarke et al., 2013) either need to have thick bark (see e.g. Midgley et al., 2011) or some other morphological adaptation to protect the meristem (e.g. see Lawes et al., 2011a, b). Investment in resprouting appears to be at the cost of seed production: in general, resprouting trees produce much less seed and therefore have a lower rate of post-disturbance establishment than non-resprouters (Midgley et al., 2010).

- 25 Aerial resprouting is found in both tropical and temperate trees, regardless of phenology (Kaufmann and Hartmann, 1991; Bellingham and Sparrow, 2000; Williams, 2000;





Bond and Midgley, 2001; Del Tredici, 2001; Paula et al., 2009). It is very uncommon in gymnosperms (Del Tredici, 2001; Paula et al., 2009; Lunt et al., 2011) and does not seem to be promoted by fire in deciduous broadleaf trees in boreal climates (Greene et al., 1999). We therefore introduced resprouting variants of four PFTs in LPX-Mv1:

5 tropical broadleaf evergreen tree (TBE), tropical broadleaf deciduous tree (TBD), temperate broadleaf evergreen tree (tBE), and temperate broadleaf deciduous tree (tBD). Parameter values were assigned to be the same as for the non-resprouting variant of each PFT, except for BT and establishment rate.

The species used in the bark thickness analysis were categorised into aerial re-sprouters, other resprouters and non-resprouters (see Table A1) based on field observations by the original data contributors, trait databases (e.g. <http://www.landmanager.org.au>; Kattge et al., 2011; Paula et al., 2009) or information in the literature (e.g. Harrison et al., 2014; Malanson and Westman, 1985; Pausas, 1997; Dagit, 2002; Tapias et al., 2004; Keeley, 2006).

15 Resprouting is facultative, and whether it is observed in a given species at a given site may depend on the fire regime and fire history of that site. Any species that was observed to resprout in one location was assumed to be capable of resprouting, even if it was classified as a non-resprouter in some studies. The range of BT for each resprouting (RS) PFT was calculated as in Sect. 3.5 (see Fig. 4 and Table 1). The 20 range of BT was also re-assigned for their non-resprouting (NR) counterparts using species classified as having no resprouting ability.

The BT and post-fire mortality of RS PFTs is calculated in the same way as for NR PFTs. The allocation of fire-killed material in RS PFTs to fuel classes is also the same as for NR PFTs. However, after fire events, the RS PFTs are not killed, as described in Eq. (7), but allowed to resprout. The new average plant for RS PFTs is calculated as the average of trees not affected by fire and fire-affected trees RS trees.

25 Seeding recruitment after disturbance is contingent on many environmental factors. Few studies have compared post-disturbance seedling recruitment by resprouters and non-resprouters, and there is no standardized reporting of environmental conditions

or responses in those studies that do exist. However, most studies show that post-disturbance (and particularly post-fire) recruitment by resprouters is lower than by non-resprouters (see e.g. Table 3). Some studies show no differences in initial recruitment (e.g. Knox and Clarke, 2006), although non-resprouters may show strategies that ensure more recruitment over a number of years (e.g. Zammit and Westoby, 1987). More systematic studies are required to characterise quantitatively the difference between resprouters and non-resprouters, but it would appear that reducing the recruitment of resprouters to ca. 10 % of that of non-resprouters is conservative. We therefore set the establishment rate of all resprouting PFTs to 10 % of that of the equivalent non-resprouting PFT.

## 4 Model configuration and test

Each change in parameterisation was implemented and evaluated separately. For each change, the model was spun-up until the carbon pools were in equilibrium. The length of the spin-up varies but is always more than 5000 yr. After spin-up, the model was run using a monthly lightning climatology from the Lightning Imaging Sensor–Optical Transient Detector High Resolution flash count ([http://gcmd.nasa.gov/records/GCMD\\_lohrmc.html](http://gcmd.nasa.gov/records/GCMD_lohrmc.html)), time-varying climate data derived from the CRU (Mitchell and Jones, 2005) and National Centers for Environmental Prediction (NCEP) reanalysis wind (NOAA Climate Diagnostics Center, Boulder, Colorado, <http://www.cdc.noaa.gov/>) data sets as described in Prentice et al. (2011). We took the opportunity to correct an error in the NCEP wind inputs used by Kelley et al. (2013), but the effects of this change were small.

We used the benchmarking system of Kelley et al. (2013) to evaluate the impacts of each change on the simulation of fire and vegetation processes. This benchmarking system quantifies differences between model outputs and observations using remotely-sensed and ground observations of a suite of vegetation and fire variables and specifically designed metrics to provide a “performance score”. We make the comparison

**Parameterisation of fire in LPX1 vegetation model**

D. I. Kelley et al.

[Title Page](#)[Abstract](#)[Introduction](#)[Conclusions](#)[References](#)[Tables](#)[Figures](#)[◀](#)[▶](#)[Back](#)[Close](#)[Full Screen / Esc](#)[Printer-friendly Version](#)[Interactive Discussion](#)

only for the continent of Australia, since this is a highly fire-prone region (van der Werf et al., 2008; Giglio et al., 2010; Bradstock et al., 2012) and was the worst simulated in the original model (see Table 7). We used the benchmark observational datasets described in Kelley et al. (2013), with the exception of CO<sub>2</sub> concentrations, runoff, GPP and NPP. There are too few data points (< 10) from Australia in the runoff, GPP and NPP datasets to make comparisons statistically meaningful. We did not use the CO<sub>2</sub> concentrations because this requires global fluxes to be calculated.

We have expanded the Kelley et al. (2013) benchmarking system to include Australia-specific datasets for production and fire (Table 4). To benchmark production, we compared modelled 1 h fuel production to the Vegetation and Soil-carbon Transfer (VAST) fine litter production dataset for Australian grassland ecosystems (Barrett, 2001). Kelley et al. (2013) provide a burnt area benchmark based on the third version of the Global Fire Database (GFED3; Giglio et al., 2010). This has recently been updated (GFED4: Giglio et al., 2013). We re-gridded the data for the period 1997–2006 to 0.5° resolution to serve as a benchmark for the model simulations, although we continue to use GFED3 for comparison with results from Kelley et al. (2013). We also use a burnt area product for southeastern Australia (New South Wales, Victoria and South Australia, NSW, VIC and SA respectively) which is based on ground observations of the extent of individual fires collected by State agencies (Bradstock et al., 2013). The original data are annual area burnt for the fire year (July through June: Mooney et al., 2012; Sullivan et al., 2012) for the period July 1970 to June 2009 on a 0.001° grid. These data were re-gridded to 0.5° resolution for annual average and inter-annual comparisons with simulated burnt area for July 1996 to June 2005. The Advanced Very High Resolution Radiometer (AVHRR) fire frequency dataset of Craig et al. (2002) and Maier and Russell-Smith (2012) provides information on the number of fires between 1997–2006 on a 1 km grid. We derive annual average burnt area by assuming that a cell could only be burnt once a year (i.e. annual average burnt area equals the number of fires divided by the number of years). The derived burnt area was then re-gridded to 0.5° resolution for comparison with simulated burnt area.

The difference between simulation and observation was assessed using the metrics as described in Kelley et al. (2013). Annual average and inter-annual comparisons were conducted using the Normalised Mean Error metric (NME). Seasonal length was benchmarked by calculating the concentration of the variable in one part of the year for

5 both model and observations, and comparing these concentrations with NME. Possible scores for NME run from 0 to  $\infty$ , with 0 being a perfect match. Changes in NME are directly proportional to the change in model agreement to observations, therefore a percentage improvement or degradation in model performance is obtained from the ratio of the original model to the new model score. NME takes a value of 1 when  
10 agreement is equal to that expected when the mean value of all observations is used as the model. Following Kelley et al. (2013), we describe model scores greater/less than 1 as better/worse than the “mean null model” and we also use random resampling of the observations to develop a second “randomly resampled” null model. Models are described as better/worse than randomly resampled if they were less/more than two  
15 standard deviations from the mean randomized score. The values for the randomly resampling null model for each variable are listed in Table 6.

For comparisons using NME, removing the influence of first the mean, and then the mean and variance, of both simulated and observed values allowed us to assess the performance of the mapped range and spatial (for annual average and season length  
20 comparisons) or temporal (for inter-annual) patterns for each variable using NME.

We used the Mean Phase Difference (MPD) metric to compare the timing of the season and the Manhattan Metric (Gavin et al., 2003; Cha, 2007) to compare vegetation type cover (Kelley et al., 2013). Both these metrics take the value 0 when the model agrees perfectly with the data. MPD has a maximum value of 1 when the modelled  
25 seasonal timing is completely out of phase with observations; whereas MM scores 2 when there is a perfect disagreement. Scores for the mean and random resampling null models for MM and MPD comparisons are given in Table 6.

The metric scores for each simulation were compared with the scores obtained with the original LPX (Table 7). Because many of the fire parameterisations in LPX were

## Parameterisation of fire in LPX1 vegetation model

D. I. Kelley et al.

[Title Page](#)[Abstract](#)[Introduction](#)[Conclusions](#)[References](#)[Tables](#)[Figures](#)[◀](#)[▶](#)[◀](#)[▶](#)[Back](#)[Close](#)[Full Screen / Esc](#)[Printer-friendly Version](#)[Interactive Discussion](#)

tuned to provide a reasonable simulation of fire, implementing individual improvements to these parameterisations can lead to a degradation of the simulation – we therefore use the performance scores for individual parameterisation changes only to help interpret the overall model performance. However, it only made sense to introduce resprouting once the other re-parameterisations had been made. We made a run that included all of the changes outlined above except for the inclusion of resprouting, and a second run which included resprouting. The first run is designated as LPX-Mv1-nr and the run including resprouting is designated LPX-Mv1-rs.

To assess the response of vegetation to the presence/absence of resprouting, we ran both LPX-Mv1-rs and LPX as described above for southeastern Australia woodland and forest ecosystems with  $\geq 20\%$  wood cover as determined by the International Satellite Land-Surface Climatology Project (ISLSCP) II vegetation continuous field (VCF) remotely-sensed dataset (Hall et al., 2006; DeFries and Hansen, 2009) (Fig. 8). Normal fire regimes were simulated until 1990, when a fire was forced burning 100 % of the grid cells, and killing (or causing to resprout, in the case of RS PFTs) 60 % of the plants. Fire was stopped for the rest of the simulation to assess recovery from this fire. As the proportion of individuals killed was fixed, this experiment only tested the RS scheme and not factors affecting mortality. The LPX simulation therefore serves as a test for NR PFTs in LPX-Mv1 as well. The simulated total foliage projected cover (FPC) in the years post-fire was compared against site-based remotely-sensed observations of inter-annual post-fire greening following fire in fire-prone sites with Mediterranean or humid subtropical vegetation (Fig. 7; Table 5), split into sites dominated by either RS and other fire adapted vegetation (normally Obligate Seeders – OS) as defined in Sect. 3.6 based on the dominant species listed in each study (Table 5). We also used studies from boreal areas with low fire frequency to examine the response in ecosystems where fire-response traits are uncommon (Table 5). The comparison between simulated and observed regeneration was performed using a simple regeneration index (RI) that describes the % recovery of lost Normalized Difference Vegetation Index (NDVI) at a given time,  $t$ , after an observed fire:

[Title Page](#)  
[Abstract](#) [Introduction](#)  
[Conclusions](#) [References](#)  
[Tables](#) [Figures](#)  
[◀](#) [▶](#)  
[◀](#) [▶](#)  
[Back](#) [Close](#)  
[Full Screen / Esc](#)  
[Printer-friendly Version](#)  
[Interactive Discussion](#)

<a href="#">Title Page</a>	
<a href="#">Abstract</a>	<a href="#">Introduction</a>
<a href="#">Conclusions</a>	<a href="#">References</a>
<a href="#">Tables</a>	<a href="#">Figures</a>
<a href="#">◀</a>	<a href="#">▶</a>
<a href="#">◀</a>	<a href="#">▶</a>
<a href="#">Back</a>	<a href="#">Close</a>
<a href="#">Full Screen / Esc</a>	
<a href="#">Printer-friendly Version</a>	
<a href="#">Interactive Discussion</a>	



$$RI_t = 100 \cdot \frac{QVI_t - \min QVI_{\text{postfire}}}{\overline{QVI}_{\text{prefire}}} \quad (35)$$

where  $QVI_t$  is the ratio of the vegetation index (VI) of the burnt areas at time  $t$  after a fire compared to that of either an unburnt control site or, in studies where a control site was not used, the average VI of the years immediately preceding the fire;  $\min(QVI_{\text{postfire}})$  is the minimum QVI in the years immediately following the fire; and  $\overline{QVI}_{\text{prefire}}$  is the average QVI in the years immediately preceding the fire. NDVI was the most commonly used remotely-sensed VI in the studies used for comparison. FPC has a linear relationship against NDVI (Purevdorj et al., 1998). However, this relationship differs between grass and woody plants (Xiao and Moody, 2005). As NDVI is normalised when used in Eq. (35), a direct conversion from FPC to NDVI is not necessary. Instead, we scaled for the different contributions from tree and grass, defining  $NDVI_{\text{sim}}$  based on the statistical model described in Sellers et al. (1996) and Lu and Shuttleworth (2002) (see Supplement, Eq. S1 to S4):

$$NDVI_{\text{sim}} = FPC_{\text{tree}} + 0.32 \cdot FPC_{\text{grass}} \quad (36)$$

where  $FPC_{\text{tree}}$  is the fractional cover of trees and  $FPC_{\text{grass}}$  of grasses.

A site or model simulation was considered to have recovered when vegetation cover reached 90 % of the pre-fire cover (i.e. when  $RI = 90 \%$ ). Recovery times for each site are listed in Table 5. Note that RI is a measure of the recovery of vegetation cover, not recovery in productivity or biomass. If a site or model simulation failed to recover before the end of the study, the recovery point was calculated by extending RI forward by fitting the post-fire data from the site to:

$$RI = 100 \cdot \left( 1 - \frac{1}{1 + p \cdot t} \right) \quad (37)$$

where  $p$  is the fitted parameter. The contribution of each site to the estimated mean and standard deviation of recovery time for a range of fire-adapted ecosystems was weighted based on the time since the last observation (Table 5). Sites that have observations during that time were given full weight, with weight decreasing exponentially with increasing time since the last observation.

5

## 5 Model performance

### 5.1 LPX-Mv1-nr

The simulation of annual average burnt area for Australia in LPX-Mv1-nr is more realistic than in LPX: the NME score is 0.86–0.89 (better than the mean model) compared to scores for LPX of 1.00–1.05 (performance equal to or worse than the mean model).  
10 The change in NME (Table 7) is equivalent to a 16–18 % improvement in model performance. The improvement in annual burnt area can be attributed to an improved match to the observed spatial pattern of fire and a better description of spatial variance. The improved NME scores obtained after removing the influence of the mean  
15 and variance of both model outputs and observations (step 3 in Table 7) is due to the introduction of fire into climates without a pronounced dry season, such as south-eastern Australia (Fig. 9) which results from the lightning re-parametrisation (Fig. S1). The improvement in spatial variability (step 2 in Table 7) is a result of decreased fire  
20 in the arid interior of the continent and an increase in fire in seasonally-dry areas of northern Australia (Fig. 9). The decrease in fire in fuel-limited regions of the interior is a result of a decrease in fuel load from faster fuel decomposition, resulting from the re-parameterisation of decomposition, and a decrease in grassland production resulting from the rooting depth re-parameterisation which leads to a decrease in the proportion of grass roots in the lower soil layer and increased water stress. Comparison  
25 of the simulated fine fuel production with VAST observations shows that the re-parameterisation of rooting depth improves simulation of fine tissue production by

[Title Page](#)

[Abstract](#)

[Introduction](#)

[Conclusions](#)

[References](#)

[Tables](#)

[Figures](#)

◀

▶

◀

▶

[Back](#)

[Close](#)

[Full Screen / Esc](#)

[Printer-friendly Version](#)

[Interactive Discussion](#)



**Parameterisation of fire in LPX1 vegetation model**

D. I. Kelley et al.

[Title Page](#)[Abstract](#)[Introduction](#)[Conclusions](#)[References](#)[Tables](#)[Figures](#)[Back](#)[Close](#)[Full Screen / Esc](#)[Printer-friendly Version](#)[Interactive Discussion](#)

**Parameterisation of fire in LPX1 vegetation model**

D. I. Kelley et al.

[Title Page](#)[Abstract](#)[Introduction](#)[Conclusions](#)[References](#)[Tables](#)[Figures](#)[◀](#)[▶](#)[◀](#)[▶](#)[Back](#)[Close](#)[Full Screen / Esc](#)[Printer-friendly Version](#)[Interactive Discussion](#)

but also through improved competition between trees and grasses for water, which results from the re-parameterisation of rooting depth. The degradation of the MM score for tree cover only (0.17 or LPX-Mv1-nr compared to 0.16 for LPX) is because the new model simulates slightly too much tree cover in southeastern Australia. The boundaries between closed forests and savanna in this region are still too sharp (Fig. 8).

Performance is degraded in LPX-Mv1-nr relative to LPX for annual average and inter-annual fAPAR (from 1.11 and 1.01 to 1.31 and 1.83 respectively) and cover of evergreen/deciduous types (0.29 to 0.72). fAPAR was already on average 59 % higher in LPX compared to observations (Table 7), mostly due to simulating too much tree cover in southeastern Australia (Fig. 8b). The introduction of adaptive bark thickness has caused an even higher average fAPAR value (Table 7) from the spread of woody vegetation into fire-prone areas (Fig. 8c). However, the inclusion of adaptive bark thickness helped improve the spatial pattern and variability (Table 7) from 0.71 to 0.57 by increasing tree cover in the north and by allowing a smoother transition between dense, high fAPAR forest near the coast and lower fAPAR grassland and desert in the interior. An MM comparison for phenology in areas where both LPX and LPX-Mv1-nr have woody cover shows little change in simulated phenology, with both scoring 0.29.

## 5.2 LPX-Mv1-rs

Including resprouting in LPX-Mv1 (LPX-Mv1-rs) produces a more accurate representation of the transition from forest through woodland/savanna to grassland (Fig. 8) and improves the simulations of vegetation cover by 2 % compared to LPX-Mv1-nr and tree cover by 6 %. There is also a significant improvement in phenology compared to LPX-Mv1-nr, with NME scores changing from 0.72 in LPX-Mv1-nr to 0.46 in LPX-Mv1-rs (Table 7). The simulation of burnt area also improves: the NME for LPX-Mv1-rs is 0.85–0.88 compared to 0.86–0.89 for LPX-Mv1-nr, representing an overall improvement of 1 %. This improvement is equally due to the decrease in burnt area resulting from increased tree cover in southwestern Queensland (QL) and southeastern Australia (Fig. 10).

## Parameterisation of fire in LPX1 vegetation model

D. I. Kelley et al.

[Title Page](#)

[Abstract](#)

[Introduction](#)

[Conclusions](#)

[References](#)

[Tables](#)

[Figures](#)

◀

▶

◀

▶

[Back](#)

[Close](#)

[Full Screen / Esc](#)

[Printer-friendly Version](#)

[Interactive Discussion](#)



The simulated distribution of trees in climate space is improved in LPX-Mv1-rs compared to LPX. Trees are slightly more abundant at values of  $\alpha$  (the ratio of actual to equilibrium evapotranspiration) between 0.2 and 0.4 in LPX-Mv1-rs than in LPX; while in humid climates, where  $\alpha > 0.8$ , trees are less abundant than in LPX. The simulated abundance of trees in LPX-Mv1-rs is in reasonable agreement with observations (Fig. 6)

The simulated distribution of RS dominance over NR PFTs is plausible. The observations indicate that aerial (apical and epicormic) resprouters are most abundant at intermediate moisture levels ( $\alpha$  between 0.4 and 0.6) but occur at higher moisture levels; the simulated abundance of RS is maximal at  $\alpha$  values between 0.4–0.5, and although it declines more rapidly at higher moisture levels than shown by the observations nevertheless resprouting still occurs in moist environments. RS have a competitive advantage over NR when  $\alpha$  is between 0.5 and 0.8 (Fig. S2).

The simulated regeneration after fire in RS-dominated communities in southeastern Australia is fast: NDVI<sub>sim</sub> reaches 90 % of pre-fire values within 7 yr, whereas post-fire regrowth takes 30 yr in the simulations that do not include RS (Fig. 7). Observations show that post-fire recovery in RS-dominated vegetation takes between 4–14 yr with a mean recovery time of 7 yr, whereas the recovery takes 8–16 yr (with a mean of 13 yr) in OS-dominated communities; and 7–22 yr (mean of 19) in boreal ecosystems.

## 20 6 Discussion

We have introduced new parameterisations within the LPX DGVM which improve the simulation of vegetation composition and fire regimes across the fire-prone continent of Australia. The overall improvement in performance in LPX-Mv1-rs compared to LPX is 18–19 % for burnt area; 17–38 % for inter-annual variability of fire; and 33 % for vegetation composition. These improvements result from the combination of all the new parameterisations. The introduction of individual parameterisations frequently led to a degradation of performance because LPX, in common with many other fire-enabled

DGVMs, was tuned to produce a reasonably realistic simulation of burnt area. Our approach here has been to develop realistic parameterisations based on analysis of large data sets; the model was not tuned against fire observations. Thus, we have achieved the overall improvement in model performance solely by introducing more realistic treatments of key processes. Adaptive bark thickness and post-fire aerial resprouting behaviour have not been included in DGVMs until now, although resprouting has been included in forest succession models (e.g. Loehle, 2000) and the BORFIRE stand-level fire response model (Groot et al., 2003). Adaptive bark thickness has not been included in any vegetation model before, despite the considerable variation in this trait both across and within ecosystems and the fact that the distribution of bark thicknesses within an ecosystem is known to shift with changes in fire regime. The incorporation of both processes is responsible for a significant part of the overall model improvement in LPX-Mv1-rs vs. LPX, and produces more realistic vegetation transitions from forests to woodland/savanna and, as shown by the regrowth comparisons, a more dynamically-responsive DGVM.

The rapid post-fire regeneration in RS dominated ecosystems is well reproduced using the modelling framework adopted here. However, simulated NR ecosystem recovery is slower than observations (Fig. 7). This might, at least in part, be because the model does not yet include fire-recovery strategies found in other ecosystems.

There are many other mechanisms for rapid ecosystem recovery after fire, including resprouting from basal or underground parts of trees and obligate seeding after fire (Clarke et al., 2013). We have focused on aerial resprouting because, although not numerically the most important type of response (Harrison et al., 2014), this has the fastest impact on ecosystem recovery (Crisp et al., 2011; Clarke et al., 2013) and thus the greatest potential to influence simulated carbon stocks and vegetation patterns. The recovery time of basal, collar and underground resprouters is slower, although not as slow as the time required for woody vegetation to re-establish from seed (Fig. 7). Basal/collar resprouting is particularly important in shrubs (Harrison et al., 2014), and thus it would be important to include this kind of behaviour in models that simulate

## Parameterisation of fire in LPX1 vegetation model

D. I. Kelley et al.

[Title Page](#)[Abstract](#)[Introduction](#)[Conclusions](#)[References](#)[Tables](#)[Figures](#)[◀](#)[▶](#)[Back](#)[Close](#)[Full Screen / Esc](#)[Printer-friendly Version](#)[Interactive Discussion](#)

**Parameterisation of fire in LPX1 vegetation model**

D. I. Kelley et al.

[Title Page](#)[Abstract](#)[Introduction](#)[Conclusions](#)[References](#)[Tables](#)[Figures](#)[◀](#)[▶](#)[Back](#)[Close](#)[Full Screen / Esc](#)[Printer-friendly Version](#)[Interactive Discussion](#)

shrub PFTs explicitly. The “obligate seeder” strategy (i.e. the release of seeds from canopy stores by fire or the triggering of germination of seeds stored in the soil by smoke or fire-produced chemicals) also leads to a more rapid recovery from fire than non-stimulated regeneration from seed. Obligate seeders are found in a wider range of ecosystems than resprouters, including boreal ecosystems.

The ability to include a wider range of post-fire responses is currently limited by the availability of large data sets which could be used to develop appropriate parameterisations. Synthesis of the quantitative information available from the vast number of field studies on these traits would be useful for the modelling community. A similar argument could be made for information on rooting depth: although this is a trait that varies considerably within PFTs and depending on environmental conditions (Schenk and Jackson, 2002b, 2005), lack of species-level data has prevented us from implementing an adaptive deep root fraction within LPX-Mv1.

Despite the improvement in the simulation of fire in southeastern Australia, LPX-Mv1-  
15 simulates ca 5 times more fire than observed in some parts of QLD, NSW and VIC, where, although the natural vegetation is woodland/savanna, the proportion of the land used for agriculture (crops, pasture) is high > 80 % (Klein Goldewijk et al., 2011). The overall impact of agriculture is to reduce burnt area dramatically (Archibald et al., 2009; Bowman et al., 2009). LPX masks crop area and does not allow it to burn. However,  
20 cropland also reduces fire by increasing fragmentation of the landscape (Archibald et al., 2012) and thereby preventing fires from spreading. Incorporating land fragmentation into LPX-Mv1 could provide a more realistic simulation of fire in agricultural areas, such as southeastern Australia.

We have used the benchmarking system described in Kelley et al. (2013) to assess  
25 the performance of the two new versions of LPX-Mv1 and to determine which new parameterisations contributed to improvements in performance. However, we needed to modify the existing system to take into account of the recent update of the global burnt area product (GFED4) and to improve comparisons for Australia by using alternative burnt area products and the VAST dataset for the assessment of fine fuel production.

**Parameterisation of fire in LPX1 vegetation model**

D. I. Kelley et al.

[Title Page](#)[Abstract](#)[Introduction](#)[Conclusions](#)[References](#)[Tables](#)[Figures](#)[|◀](#)[▶|](#)[◀](#)[▶|](#)[Back](#)[Close](#)[Full Screen / Esc](#)[Printer-friendly Version](#)[Interactive Discussion](#)

As pointed out by Kelley et al. (2013), the incorporation of new processes into DGVMs will require the creation of new benchmarks. We have used the conceptual framework of Clarke et al. (2013), which is based on extensive field observations, to evaluate our simulations of RS-dominance in a qualitative way. Spatially-explicit data on the distribution and abundance of resprouting species is required to test our simulations quantitatively. An Australian dataset of RS abundance in fire-prone ecosystems is currently under development (Harrison et al., 2014); it would be useful if such a dataset were available for a wider range of ecosystems and climates. Similarly, we have shown that an adaptive bark thickness parameterisation produces qualitatively plausible changes in average bark thickness in different regions and under different fire regimes, using field-based studies. A spatially-explicit database of bark thickness would enable us to test the simulated patterns in bark thickness across ecosystems and fire regimes in a quantitative way.

## 7 Conclusions

Fire-vegetation interactions involve many processes and feedbacks. It is possible to tune a model to provide the best fit to an emergent property of the fire-vegetation system, such as observed burnt area, in multiple ways. Good simulations of burnt area can be obtained through many different combinations of parameter values. Such tuning can also lead to the assignment of parameter values that are wrong. Our approach in developing new fire parameterisations for LPX-Mv1 has been to rely on the analysis of data directly relevant to each individual process. This approach is possible because of the steadily-increasing amount of data available through satellite observations and geographically-explicit syntheses of ground observations. The new model incorporates a more realistic description of fire processes and produces a better simulation of vegetation properties and fire regimes across Australia, and is expected to produce a considerable improvement in the simulation of fire-prone vegetation worldwide.

Acknowledgements. We thank Belinda Medlyn and Peter M. van Bodegom for discussion of the treatment of variable bark thickness, and Joe Fontaine, Mike Lawes, Jeremy Midgley, Peter Clarke, Zhixin Fang, Bill Hoffman, Marin Pompa-Garcia, Daniel Laughlin, Peter M. van Bodegom, Timothy Paine, Christopher Baraloto, Paulo Brando, Emily Swaine, William Bond and Jon Lloyd for provision of bark thickness data. We also thank Victor Brokin and Thomas Kleinen for providing their litter decomposition code. DIK is supported by an iMQRES at Macquarie University.

Benchmarking datasets and scripts for data-model comparison metrics from both Kelley et al. (2013) and the updates described here are available at <http://bio.mq.edu.au/bcd/benchmarks/>. Information and code used for data analysis are available at [https://bitbucket.org/teambcd/lpx2013\\_data\\_analysis](https://bitbucket.org/teambcd/lpx2013_data_analysis). Benchmarking and data analysis were scripted using R (R Development Core Team) and the quantreg (Koenker, 2013), raster (van Etten and Hijmans, 2013), glm (R Core Team, 2013), RNetCDF (Michna, 2012) and Hmisc (Harrell Jr., 2012) packages.

## References

- Albini, F. A.: Estimating wildfire behavior and effects, Intermountain Forest and Range Experiment Station, Forest Service, US Department of Agriculture, 1976. 936
- Anderson, D. H., Catchpole, E. A., De Mestre, N. J., and Parkes, T.: Modelling the spread of grass fires, *J. Aust. Math. Soc.*, 23, 451–466, 1982. 936
- Archibald, S., Roy, D. P., van Wilgen, B. W., and Scholes, R. J.: What limits fire?, an examination of drivers of burnt area in southern Africa, *Glob. Change Biol.*, 15, 613–630, doi:10.1111/j.1365-2486.2008.01754.x, 2009. 960
- Archibald, S., Staver, A. C., and Levin, S. A.: Evolution of human-driven fire regimes in Africa, *P. Natl. Acad. Sci. USA*, 109, 847–852, doi:10.1073/pnas.1118648109, 2012. 960

Title Page

Abstract

Introduction

Conclusions

References

Tables

Figures

◀

▶

Back

Close

Full Screen / Esc

Printer-friendly Version

Interactive Discussion



Baldocchi, D., Cummins, K. L., Christian, H. J., and Goodman, S. J.: Combined satellite- and surface-based estimation of the intracloud – cloud-to-ground lightning ratio over the continental United States, *Mon. Weather Rev.*, 129, 108–122, 2000. 938, 939

Barrett, D. J.: NPP multi-biome: VAST calibration data, 1965–1998, available at: <http://www.daac.ornl.gov> (last access: 13 January 2011), 2001. 951, 979

Bellingham, P. J. and Sparrow, A. D.: Resprouting as a life history strategy in woody plant communities, *Oikos*, 89, 409–416, 2000. 945, 948

Biganzoli, F., Wiegand, T., and Batista, W. B.: Fire-mediated interactions between shrubs in a South American temperate savannah, *Oikos*, 118, 1383–1395, doi:10.1111/j.1600-0706.2009.17349.x, 2009. 933, 978

Bond, W. J. and Midgley, J. J.: Ecology of sprouting in woody plants: the persistence niche, *Trends Ecol. Evol.*, 16, 45–51, 2001. 945, 949

Bond, W. J. and Van Wilgen, B. W.: *Fire and Plants, Population and Community Biology Series*, 14, 1996. 933

Bowman, D. M. J. S., Balch, J. K., Artaxo, P., Bond, W. J., Carlson, J. M., Cochrane, M. a., D'Antonio, C. M., Defries, R. S., Doyle, J. C., Harrison, S. P., Johnston, F. H., Keeley, J. E., Krawchuk, M. A., Kull, C. A., Marston, J. B., Moritz, M. A., Prentice, I. C., Roos, C. I., Scott, A. C., Swetnam, T. W., van der Werf, G. R., and Pyne, S. J.: Fire in the earth system, *Science* (New York, N. Y.), 324, 481–484, doi:10.1126/science.1163886, 2009. 960

Bradstock, R., Williams, R., and Gill, A.: *Flammable Australia: Fire Regimes, Biodiversity and Ecosystems in a Changing World*, CSIRO Publishing, 2012. 951

Bradstock, R., Penman, T., Boer, M., Price, O., and Clarke, H.: Divergent responses of fire to recent warming and drying across south-eastern Australia, *Glob. Change Biol.*, online first, doi:10.1111/gcb.12449, 2013. 951, 979, 999

Brando, P. M., Nepstad, D. C., Balch, J. K., Bolker, B., Christman, M. C., Coe, M., and Putz, F. E.: Fire-induced tree mortality in a neotropical forest: the roles of bark traits, tree size, wood density and fire behavior, *Glob. Change Biol.*, 18, 630–641, doi:10.1111/j.1365-2486.2011.02533.x, 2012. 945

Brokin, V., van Bodegom, P. M., Kleinen, T., Wirth, C., Cornwell, W. K., Cornelissen, J. H. C., and Kattge, J.: Plant-driven variation in decomposition rates improves projections of global litter stock distribution, *Biogeosciences*, 9, 565–576, doi:10.5194/bg-9-565-2012, 2012. 943

Calvo, L., Santalla, S., Marcos, E., Valbuena, L., Tárrega, R., and Luis, E.: Regeneration after wildfire in communities dominated by *Pinus pinaster*, an obligate seeder, and in others

[Title Page](#)

[Abstract](#)

[Introduction](#)

[Conclusions](#)

[References](#)

[Tables](#)

[Figures](#)

◀

▶

[Back](#)

[Close](#)

[Full Screen / Esc](#)

[Printer-friendly Version](#)

[Interactive Discussion](#)



dominated by *Quercus pyrenaica*, a typical resprouter, Forest Ecol. Manag., 184, 209–223, doi:10.1016/S0378-1127(03)00207-X, 2003. 948

Casady, G.: Examining Drivers of Post-Wildfire Vegetation Dynamics Across Multiple Scales Using Time-Series Remote Sensing, ProQuest, 2008. 948

5 Casady, G. M., van Leeuwen, W. J. D., and Marsh, S. E.: Evaluating post-wildfire vegetation regeneration as a response to multiple environmental determinants, Environ. Model. Assess., 15, 295–307, doi:10.1007/s10666-009-9210-x, 2009. 948, 982

10 Cha, S.-H.: Comprehensive survey on distance/similarity measures between probability density functions, International Journal of Mathematical Models and Methods in applied sciences, 4, 300–307, 2007. 952

Chave, J., Coomes, D., Jansen, S., Lewis, S. L., Swenson, N. G., and Zanne, A. E.: Towards a worldwide wood economics spectrum, Ecol. Lett., 12, 351–366, doi:10.1111/j.1461-0248.2009.01285.x, 2009. 943

15 Christian, H. J.: Optical detection of lightning from space, in: Proceedings of the 11th International Conference on Atmospheric Electricity, Guntersville, Alabama, 715–718, 1999. 938, 992

20 Christian, H. J., Blakeslee, R. J., Goodman, S. J., Mach, D. A., Stewart, M. F., Buechler, D. E., Koshak, W. J., Hall, J. M., Boeck, W. L., Driscoll, K. T., and Bocippio, D. J.: The lightning imaging sensor, in: Proceedings of the 11th International Conference On Atmospheric Electricity, Guntersville, Alabama, 746–749, 1999. 938, 992

Clarke, P. J., Lawes, M. J., Midgley, J. J., Lamont, B. B., Ojeda, F., Burrows, G. E., Enright, N. J., and Knox, K. J. E.: Resprouting as a key functional trait: how buds, protection and resources drive persistence after fire, New Phytol., 197, 19–35, doi:10.1111/nph.12001, 2013. 934, 948, 959, 961

25 Climent, J., Tapias, R., Pardos, J. A., and Gil, L.: Fire adaptations in the Canary Islands pine (*Pinus canariensis*), Plant Ecol., 171, 185–196, 2004. 945

Cochrane, M. A.: Fire science for rainforests, Nature, 421, 913–919, doi:10.1038/nature01437, 2003. 945

30 Cornwell, W. K., Cornelissen, J. H. C., Amatangelo, K., Dorrepaal, E., Eviner, V. T., Godoy, O., Hobbie, S. E., Hoorens, B., Kurokawa, H., Pérez-Harguindeguy, N., Quested, H. M., Santiago, L. S., Wardle, D. A., Wright, I. J., Aerts, R., Allison, S. D., van Bodegom, P., Brovkin, V., Chatain, A., Callaghan, T. V., Díaz, S., Garnier, E., Gurvich, D. E., Kazakou, E., Klein, J. A., Read, J., Reich, P. B., Soudzilovskaia, N. A., Vaieretti, M. V., and Westoby, M.: Plant species

[Title Page](#)

[Abstract](#)

[Introduction](#)

[Conclusions](#)

[References](#)

[Tables](#)

[Figures](#)

◀

▶

[Back](#)

[Close](#)

[Full Screen / Esc](#)

[Printer-friendly Version](#)

[Interactive Discussion](#)



traits are the predominant control on litter decomposition rates within biomes worldwide, Ecol. Lett., 11, 1065–71, doi:10.1111/j.1461-0248.2008.01219.x, 2008. 943

5 Cornwell, W. K., Cornelissen, J. H. C., Allison, S. D., Bauhus, J., Eggleton, P., Preston, C. M., Scarff, F., Weedon, J. T., Wirth, C., and Zanne, A. E.: Plant traits and wood fates across the globe: rotted, burned, or consumed?, Glob. Change Biol., 15, 2431–2449, doi:10.1111/j.1365-2486.2009.01916.x, 2009. 943

10 Craig, R., Heath, B., Raisbeck-Brown, N., Steber, M., Marsden, J., and Smith, R.: The distribution, extent and seasonality of large fires in Australia, April 1998–March 2000, as mapped from NOAA-AVHRR imagery, in: Australian fire regimes: contemporary patterns (April 1998 – March 2000) and Changes since European settlement, edited by: Russell-Smith, J., Craig, R., Gill, A. M., Smith, R., and Williams, J., (March), Department of the Environment and Heritage, Canberra, available at: <http://laptop.deh.gov.au/soe/2001/publications/technical/fire/pubs/part1.pdf> (last access: 7 June 2013), 2002. 951

15 Crisp, M. D., Burrows, G. E., Cook, L. G., Thornhill, A. H., and Bowman, D. M. J. S.: Flammable biomes dominated by eucalypts originated at the Cretaceous-Palaeogene boundary, Nature Com., 2, 193, doi:10.1038/ncomms1191, 2011. 959

Cuevas-González, M., Gerard, F., Balzter, H., and Riaño, D.: Analysing forest recovery after wildfire disturbance in boreal Siberia using remotely sensed vegetation indices, Glob. Change Biol., 15, 561–577, doi:10.1111/j.1365-2486.2008.01784.x, 2009. 982

20 Cummins, K. and Murphy, M.: An overview of lightning locating systems: history, techniques, and data uses, with an in-depth look at the US NLDN, electromagnetic compatibility, IEEE, 51, 499–518, 2009. 938, 939, 992

Dagit, R.: Post-fire monitoring of coast live Oaks (*Quercus agrifolia*) burned in the 1993 Old Topanga fire, Proceedings of the Fifth Natural Resources, 90290, 243–249, 2002. 949

25 de Souza, P. E., Pinto, O., Pinto, I. R. C. A., Ferreira, N. J., and Dos Santos, A. F.: The intracloud/cloud-to-ground lightning ratio in southeastern Brazil, Atmos. Res., 91, 491–499, 2009. 938

30 DeFries, R. and Hansen, M.: ISLSCP II Continuous fields of vegetation cover, 1992–1993, in: ISLSCP Initiative II Collection, edited by: Hall, F., Collatz, G., Brown de Colstoun, E., Landis, D., Los, S., and Meeson, B., Oak Ridge National Laboratory Distributed Active Archive Center, Oak Ridge, Tennessee, USA, doi:10.3334/ORNLDAAC/931, 2009. 953, 979, 996, 998

Parameterisation of  
fire in LPX1  
vegetation model

D. I. Kelley et al.

Title Page

Abstract

Introduction

Conclusions

References

Tables

Figures

◀

▶

Back

Close

Full Screen / Esc

Printer-friendly Version

Interactive Discussion



- Del Tredici, P.: Sprouting in temperate trees: a morphological and ecological review, *Bot. Rev.*, 67, 121–140, 2001. 945, 949
- Díaz-Delgado, R., Salvador, R., and Pons, X.: Monitoring of plant community regeneration after fire by remote sensing, *Fire Manage. Landsc. Ecol.*, 315–324, 1998. 981
- 5 Díaz-Delgado, R., Loreto, F., Pons, X., and Terradas, J.: Satellite evidence of decreasing resilience in mediterranean plant communities after recurrent wildfires, *Ecol. Soc. Am.*, 83, 2293–2303, 2002. 981
- Díaz-Delgado, R., Lloret, F., and Pons, X.: Influence of fire severity on plant regeneration by means of remote sensing imagery, *J. Remote Sens.*, 24, 1751–1763, 2003. 982
- 10 Enright, N. J. and Goldblum, D.: Demography of a non-sprouting and resprouting Hakea species (*Proteaceae*) in fire-prone Eucalyptus woodlands of southeastern Australia in relation to stand age, drought and disease, *Plant Ecol.*, 144, 71–82, 1999. 978
- Enright, N. J. and Lamont, B. B.: Seed banks, fire season, safe sites and seedling recruitment in five co-occurring Banksia species, *J. Ecol.*, 77, 1111–1122, 1989. 978
- 15 Epting, J. and Verbyla, D.: Landscape-level interactions of prefire vegetation, burn severity, and postfire vegetation over a 16-year period in interior Alaska, *Can. J. Forest Res.*, 1377, 1367–1377, doi:10.1139/X05-060, 2005. 982
- Foley, J.: An equilibrium model of the terrestrial carbon budget, *Tellus B*, 47, 310–319, 1995. 935
- 20 Friend, A. D.: Parameterisation of a global daily weather generator for terrestrial ecosystem modelling, *Ecol. Model.*, 109, 121–140, doi:10.1016/S0304-3800(98)00036-2, 1998. 941
- Fyllas, N. M., Patiño, S., Baker, T. R., Bielefeld Nardoto, G., Martinelli, L. A., Quesada, C. A., Paiva, R., Schwarz, M., Horna, V., Mercado, L. M., Santos, A., Arroyo, L., Jiménez, E. M., Luizão, F. J., Neill, D. A., Silva, N., Prieto, A., Rudas, A., Silviera, M., Vieira, I. C. G., Lopez-Gonzalez, G., Malhi, Y., Phillips, O. L., and Lloyd, J.: Basin-wide variations in foliar properties of Amazonian forest: phylogeny, soils and climate, *Biogeosciences*, 6, 2677–2708, doi:10.5194/bg-6-2677-2009, 2009. 945
- 25 Gallego-Sala, A. V., Clark, J. M., House, J. I., Orr, H. G., Prentice, I. C., Smith, P., Farewell, T., and Chapman, S. J.: Bioclimatic envelope model of climate change impacts on blanket peatland distribution in Great Britain, *Clim. Res.*, 45, 151–162, 2010. 996
- Gavin, D. G., Oswald, W. W., Wahl, E. R., and Williams, J. W.: A statistical approach to evaluating distance metrics and analog assignments for pollen records, *Quaternary Res.*, 60, 356–367, 2003. 952

## Parameterisation of fire in LPX1 vegetation model

D. I. Kelley et al.

[Title Page](#)[Abstract](#)[Introduction](#)[Conclusions](#)[References](#)[Tables](#)[Figures](#)[◀](#)[▶](#)[◀](#)[▶](#)[Back](#)[Close](#)[Full Screen / Esc](#)[Printer-friendly Version](#)[Interactive Discussion](#)



## Parameterisation of fire in LPX1 vegetation model

D. I. Kelley et al.

[Title Page](#)

[Abstract](#)

[Introduction](#)

[Conclusions](#)

[References](#)

[Tables](#)

[Figures](#)

◀

▶

[Back](#)

[Close](#)

[Full Screen / Esc](#)

[Printer-friendly Version](#)

[Interactive Discussion](#)



- Harrell Jr., F. E.: Hmisc: Harrell miscellaneous, available at: <http://cran.r-project.org/package=Hmisc> (last access: 16 December 2013), 2012. 962
- Harris, I., Jones, P. D., Osborn, T. J., and Lister, D. H.: Updated high-resolution grids of monthly climatic observations – the CRU TS3.10 Dataset, *Int. J. Climatol.*, doi:10.1002/joc.3711, 2013. 939, 944
- Harrison, S. P., Prentice, I. C., Barboni, D., Kohfeld, K. E., Ni, J., and Sutra, J.-P.: Ecophysiological and bioclimatic foundations for a global plant functional classification, *J. Veg. Sci.*, 21, 300–317, doi:10.1111/j.1654-1103.2009.01144.x, 2010. 944
- Harrison, S., Kelley, D., Wang, H., Herbert, A., Li, G., Bradstock, R., Fontaine, J., Enright, N., Murphy, B., Penman, T., and Russell-Smith, J.: Patterns in fire-response trait abundances in Australia using a new database of plot-level measurements for fire model evaluation, *Int. J. Wildland Fire*, submitted, 2014. 949, 959, 961, 996
- Hastie, T. J. and Pregibon, D.: Generalized linear models, Chapter 6 of *Statistical Models in S*, edited by: Chambers, J. M. and Hastie, T. J., Wadsworth & Brooks/Cole, 1992. 939
- Higgins, R. W. and Centre, U. C. P.: Improved United States precipitation quality control system and analysis, in: NCEP/Climate Prediction Center ATLAS No. 6, NOAA, National Weather Service, National Centers for Environmental Prediction, Climate Prediction Center, Camp Springs, MD, 2000. 939
- Higgins, R. W., Janowiak, J. E., and Yao, Y.-P.: A gridded hourly precipitation data base for the United States (1963–1993), in: NCEP/Climate prediction center atlas 1, p. 46, NOAA, National Weather Service, National Centers for Environmental Prediction, Climate Prediction Center, Camp Springs, MD, 1996. 939
- Hijmans, R. J., Cameron, S. E., Parra, J. L., Jones, P. G., and Jarvis, A.: Very high resolution interpolated climate surfaces for global land areas, *Int. J. Climatol.*, 25, 1965–1978, 2005. 939
- Hope, A., Tague, C., and Clark, R.: Characterizing post fire vegetation recovery of California chaparral using TM and ETM timeseries data, *Int. J. Remote Sens.*, 28, 1339–1354, doi:10.1080/01431160600908924, 2007. 981
- Kattge, J., Diaz, S., Lavorel, S., Prentice, I. C., Leadley, P., Bonisch, G., Garnier, E., Westoby, M., Reich, P. B., Wright, I. J., CornNeilissen, J. H. C., Violle, C., Harrison, S. P., Van Bodegom, P. M., Reichstein, M., Enquist, B. J., Soudzilovskaya, N. A., Ackerly, D. D., Anand, M., Atkin, O., Bahn, M., Baker, T. R., Baldocchi, D., Bekker, R., Blanco, C. C., Blonder, B., Bond, W. J., Bradstock, R., Bunker, D. E., Casanoves, F., Cavender-Bares, J.,

## Parameterisation of fire in LPX1 vegetation model

D. I. Kelley et al.

[Title Page](#)

[Abstract](#)

[Introduction](#)

[Conclusions](#)

[References](#)

[Tables](#)

[Figures](#)

◀

▶

[Back](#)

[Close](#)

[Full Screen / Esc](#)

[Printer-friendly Version](#)

[Interactive Discussion](#)



Chambers, J. Q., Chapin III, F. S., Chave, J., Coomes, D., Cornwell, W. K., Craine, J. M., Dobrin, B. H., Duarte, L., Durka, W., Elser, J., Esser, G., Estiarte, M., Fagan, W. F., Fang, J., Fernandez-Mendez, F., Fidelis, A., Finegan, B., Flores, O., Ford, H., Frank, D., Freschet, G. T., Fyllas, N. M., Gallagher, R. V., Green, W. A., Gutierrez, A. G., Hickler, T., Higgins, S. I., Hodgson, J. G., Jalili, A., Jansen, S., Joly, C. A., Kerkhoff, A. J., Kirkup, D., Kitajima, K., Kleyer, M., Klotz, S., Knops, J. M. H., Kramer, K., Kuhn, I., Kurokawa, H., Laughlin, D., Lee, T. D., Leishman, M., Lens, F., Lenz, T., Lewis, S. L., Lloyd, J., Llusia, J., Louault, F., Ma, S., Mahecha, M. D., Manning, P., Massad, T., Medlyn, B. E., Messier, J., Moles, A. T., Muller, S. C., Nadrowski, K., Naeem, S., Niinemets, U., Nollert, S., Nuske, A., Ogaya, R., Oleksyn, J., Onipchenko, V. G., Onoda, Y., Ordonez, J., Overbeck, G., Ozinga, W. A., Patino, S., Paula, S., Pausas, J. G., Penuelas, J., Phillips, O. L., Pillar, V., Poorter, H., Poorter, L., Poschlod, P., Prinzing, A., Proulx, R., Rammig, A., Reinsch, S., Reu, B., Sack, L., Salgado-Negret, B., Sardans, J., Shiodera, S., Shipley, B., Siefert, A., Sosinski, E., Sousiana, J.-F., Swaine, E., Swenson, N., Thompson, K., Thornton, P., Waldram, M., Weiher, E., White, M., White, S., Wright, S. J., Yguel, B., Zaeble, S., Zanne, A. E., and Wirth, C.: TRY – a global database of plant traits, *Glob. Change Biol.*, 17, 2905–2935, doi:10.1111/j.1365-2486.2011.02451.x, 2011. 943, 949

Kauffman, J. B.: Survival by sprouting following fire in tropical forests of the eastern Amazon, *Biotropica*, 23, 219–224, 1991. 945

Kaufmann, W. F. and Hartmann, K. M.: Earth-based spectroradiometric monitoring of forest decline, *J. Plant Physiol.*, 138, 270–273, 1991. 948

Keeley, J. E.: Fire severity and plant age in postfire resprouting of woody plants in sage scrub and chaparral, *Madrono*, 53, 373–379, 2006. 949

Kelley, D. I., Prentice, I. C., Harrison, S. P., Wang, H., Simard, M., Fisher, J. B., and Willis, K. O.: A comprehensive benchmarking system for evaluating global vegetation models, *Biogeosciences*, 10, 3313–3340, doi:10.5194/bg-10-3313-2013, 2013. 933, 934, 950, 951, 952, 960, 961

Kimball, J. S., Running, S. W., and Nemani, R.: An improved method for estimating surface humidity from daily minimum temperature, *Agr. Forest Meteorol.*, 1997. 942, 943

Klein Goldewijk, K., Beusen, A., Van Drecht, G., and De Vos, M.: The HYDE 3.1 spatially explicit database of human-induced global land-use change over the past 12,000 years, *Global Ecol. Biogeogr.*, 20, 73–86, 2011. 960

Knox, K. J. E. and Clarke, P. J.: Fire season and intensity affect shrub recruitment in temperate sclerophyllous woodlands, *Oecologia*, 149, 730–739, doi:10.1007/s00442-006-0480-6, 2006. 950

Koenker, R.: Package “quantreg”: quantile regression, available at: <http://cran.r-project.org/package=quantreg> (last access: 6 December 2013), 2013. 946, 962

Kuleshov, Y. and Jayaratne, R.: Estimates of lightning ground flash density in Australia and its relationship to thunder-days, *Aust. Meteorol. Mag.*, 53, 189–196, 2004. 938

Lawes, M. J., Adie, H., Russell-Smith, J., Murphy, B., and Midgley, J. J.: How do small savanna trees avoid stem mortality by fire? The roles of stem diameter, height and bark thickness, *Ecosphere*, 2, 42, doi:10.1890/ES10-00204.1, 2011a. 945, 948

Lawes, M. J., Richards, A., Dathe, J., and Midgley, J. J.: Bark thickness determines fire resistance of selected tree species from fire-prone tropical savanna in north Australia, *Plant Ecol.*, 212, 2057–2069, doi:10.1007/s11258-011-9954-7, 2011b. 948

Lawrence, M. G.: The relationship between relative humidity and the dewpoint temperature in moist air: a simple conversion and applications, *B. Am. Meteorol. Soc.*, 86, 225–233, doi:10.1175/BAMS-86-2-225, 2005. 942

Lehmann, C. E. R., Prior, L. D., Williams, R. J., and Bowman, D. M. J. S.: Spatio-temporal trends in tree cover of a tropical mesic savanna are driven by landscape disturbance, *J. Appl. Ecol.*, 45, 1304–1311, doi:10.1111/j.1365-2664.2008.01496.x, 2008. 933

Lloyd, J. and Taylor, J.: On the temperature dependence of soil respiration, *Funct. Ecol.*, 8, 315–323, 1994. 935

Loehle, C.: Strategy space and the disturbance spectrum: a life-history model for tree species coexistence, *Am. Nat.*, 156, 14–33, 2000. 959

Lu, L. and Shuttleworth, J. W.: Incorporating NDVI-Derived LAI into the climate version of RAMS and its impact on regional climate, *J. Hydrometeorol.*, 3, 347–362, 2002. 954

Lunt, I. D., Zimmer, H. C., and Cheal, D. C.: The tortoise and the hare? Post-fire regeneration in mixed Eucalyptus–Callitris forest, *Aust. J. Bot.*, 59, 575–581, 2011. 945, 949

Maier, S. W. and Russell-Smith, J.: Measuring and monitoring of contemporary fire regimes in Australia using satellite remote sensing, in: *Flammable Australia: Fire Regimes, Biodiversity and Ecosystems in a Changing World*, edited by: Bradstock, R., Williams, R., and Gill, A., 79–95, CSIRO Publishing, 2012. 951, 979, 999

Title Page

Abstract

Introduction

Conclusions

References

Tables

Figures

◀

▶

◀

▶

Back

Close

Full Screen / Esc

Printer-friendly Version

Interactive Discussion



## Parameterisation of fire in LPX1 vegetation model

D. I. Kelley et al.

[Title Page](#)

[Abstract](#)

[Introduction](#)

[Conclusions](#)

[References](#)

[Tables](#)

[Figures](#)

◀

▶

[Back](#)

[Close](#)

[Full Screen / Esc](#)

[Printer-friendly Version](#)

[Interactive Discussion](#)



Malanson, G. P. and Westman, W. E.: Postfire succession in Californian coastal Sage scrub: the role of continual Basal sprouting, Am. Midl. Nat., 113, 309–318, doi:10.2307/2425576, 1985. 949

Michna, P.: RNetCDF: R Interface to NetCDF Datasets, available at: <http://cran.r-project.org/package=RNetCDF> (last access: 6 December 2013), 2012. 962

Midgley, J. J., Lawes, M. J., and Chamaillé-Jammes, S.: Turner Review No. 19. Savanna woody plant dynamics: the role of fire and herbivory, separately and synergistically, Austr. J. Bot., 58, 1–11, doi:10.1071/BT09034, 2010. 948

Midgley, J., Kruger, L., and Skelton, R.: How do fires kill plants? The hydraulic death hypothesis and Cape Proteaceae “fire-resisters”, S. Afr. J. Bot., 77, 381–386, doi:10.1016/j.sajb.2010.10.001, 2011. 948

Mitchell, T. D. and Jones, P. D.: An improved method of constructing a database of monthly climate observations and associated high-resolution grids, Int. J. Climatol., 25, 693–712, doi:10.1002/joc.1181, 2005. 950

Mooney, S. D., Harrison, S. P., Bartlein, P. J., and Stevenson, J.: The prehistory of fire in Australasia, in: Flammable Australia: fire regimes, biodiversity and ecosystems in a changing world, edited by: Bradstock, R., Gill, A., and Williams, R., 3–25, CSIRO Publishing, 2012. 951

Murray, L. T., Jacob, D. J., Logan, J. A., Hudman, R. C., and Koshak, W. J.: Optimized regional and interannual variability of lightning in a global chemical transport model constrained by LIS/OTD satellite data, J. Geophys. Res.-Atmos., 117, D20307, doi:10.1029/2012JD017934, 2012. 940

Nesterov, V. G.: Combustibility of the forest and methods for its determination, Goslesbumaga, Moscow, 1949. 936

Paine, C. E. T., Stahl, C., Courtois, E. A., Patiño, S., Sarmiento, C., and Baraloto, C.: Functional explanations for variation in bark thickness in tropical rain forest trees, Funct. Ecol., 24, 1202–1210, doi:10.1111/j.1365-2435.2010.01736.x, 2010. 945

Paula, S., Arianoutsou, M., Kazanis, D., Tavsanoglu, C., Lloret, F., Buhk, C., Ojeda, F., Luna, B., Moreno, J. M., Rodrigo, A., Espelta, J. M., Pausas, J. G., Fernández-Santos, B., Fernandes, P. M., and Pausas, J. G.: Fire-related traits for plant species of the Mediterranean Basin, Ecol., 90, 1420 pp., 2009. 945, 949

Pausas, J. G.: Resprouting of *Quercus suber* in NE Spain after fire, J. Veg. Sci., 8, 703–706, 1997. 949

## Parameterisation of fire in LPX1 vegetation model

D. I. Kelley et al.

[Title Page](#)

[Abstract](#)

[Introduction](#)

[Conclusions](#)

[References](#)

[Tables](#)

[Figures](#)

◀

▶

[Back](#)

[Close](#)

[Full Screen / Esc](#)

[Printer-friendly Version](#)

[Interactive Discussion](#)



## Parameterisation of fire in LPX1 vegetation model

D. I. Kelley et al.

<a href="#">Title Page</a>	
<a href="#">Abstract</a>	<a href="#">Introduction</a>
<a href="#">Conclusions</a>	<a href="#">References</a>
<a href="#">Tables</a>	<a href="#">Figures</a>
<a href="#">◀</a>	<a href="#">▶</a>
<a href="#">◀</a>	<a href="#">▶</a>
<a href="#">Back</a>	<a href="#">Close</a>
<a href="#">Full Screen / Esc</a>	
<a href="#">Printer-friendly Version</a>	
<a href="#">Interactive Discussion</a>	



Schenk, H. J. and Jackson, R. B.: Rooting depths, lateral root spreads and belowground above-ground allometries of plants in water limited ecosystems, *J. Ecol.*, 90, 480–494, 2002a. 944, 993

Schenk, H. J. and Jackson, R. B.: The global biogeography of roots, *Ecol. Monogr.*, 72, 311–328, 2002b. 944, 945, 960

Schenk, H. J. and Jackson, R. B.: Mapping the global distribution of deep roots in relation to climate and soil characteristics, *Geoderma*, 126, 129–140, doi:10.1016/j.geoderma.2004.11.018, 2005. 944, 960, 993

Sellers, P. J., Tucker, C. J., Collatz, G. J., Los, S. O., Justice, C. O., Dazlich, D. A., and Randall, D. A.: A revised land surface parameterization (SiB2) for atmospheric GCMs, Part II: The generation of global fields of terrestrial biophysical parameters from satellite data, *J. Climate*, 4, 706–737, 1996. 954

Sharples, J. J., McRae, R. H. D., Weber, R. O., and Gill, A. M.: A simple index for assessing fuel moisture content, *Environ. Modell. Softw.*, 24, 637–646, doi:10.1016/j.envsoft.2008.10.012, 2009. 941, 942

Silva-Matos, D. M., Fonseca, G. D. F. M., and Silva-Lima, L.: Differences on post-fire regeneration of the pioneer trees *Cecropia glazioui* and *Trema micrantha* in a lowland Brazilian Atlantic forest, *Revista de biología tropical*, 53, 1–4, 2005. 978

Simard, M., Baccini, A., Fisher, J. B., and Pinto, N.: Mapping forest canopy height globally with spaceborne lidar, *J. Geophys. Res.*, 116, G04021, doi:10.1029/2011JG001708, 2011. 979

Sitch, S., Smith, B., Prentice, I. C., Arneth, A., Bondeau, A., Cramer, W., Kaplan, J. O., Levis, S., Lucht, W., Sykes, M. T., Thonikke, K., and Venevsky, S.: Evaluation of ecosystem dynamics, plant geography and terrestrial carbon cycling in the LPJ dynamic global vegetation model, *Glob. Change Biol.*, 9, 161–185, 2003. 935

Solans Vila, J. P. and Barbosa, P.: Post-fire vegetation regrowth detection in the Deiva Marina region (Liguria-Italy) using Landsat TM and ETM+ data, *Ecol. Model.*, 221, 75–84, doi:10.1016/j.ecolmodel.2009.03.011, 2010. 982

Sullivan, A. L., McCaw, W. L., Cruz, M. G., Matthews, S., and Ellis, P. F.: Fuel, fire weather and fire behaviour in Australian ecosystems, in: *Flammable Australia: Fire Regimes, Biodiversity and Ecosystems in a Changing World*, edited by: Bradstock, R., Gill, A., and Williams, R., 51–79, CSIRO Publishing, 2012. 951

Tapias, R., Climent, J., Pardos, J. A., and Gil, L.: Life histories of Mediterranean pines, *Plant Ecol.*, 171, 53–68, 2004. 949

- Thonicke, K., Spessa, A., Prentice, I. C., Harrison, S. P., Dong, L., and Carmona-Moreno, C.: The influence of vegetation, fire spread and fire behaviour on biomass burning and trace gas emissions: results from a process-based model, *Biogeosciences*, 7, 1991–2011, doi:10.5194/bg-7-1991-2010, 2010. 934, 935, 936, 937
- 5 van der Werf, G. R., Randerson, J. T., Giglio, L., Gobron, N., and Dolman, A. J.: Climate controls on the variability of fires in the tropics and subtropics, *Global Biogeochem. Cy.*, 22, GB3028, doi:10.1029/2007GB003122, 2008. 933, 951
- van Etten, J. and Hijmans, R. J.: raster: Geographic data analysis and modeling, available at: <http://cran.r-project.org/package=raster> (last access: 16 December 2013), 2013. 962
- 10 van Leeuwen, W. J. D.: Monitoring the effects of forest restoration treatments on post-fire vegetation recovery with MODIS multitemporal data, *Sensors*, 8, 2017–2042, doi:10.3390/s8032017, 2008. 982
- van Leeuwen, W. J. D., Casady, G. M., Neary, D. G., Bautista, S., Alloza, J. A., Carmel, Y.,  
15 Wittenberg, L., Malkinson, D., and Orr, B. J.: Monitoring post-wildfire vegetation response with remotely sensed time-series data in Spain, USA and Israel, *Int. J. Wildland Fire*, 19, 75–93, doi:10.1071/WF08078, 2010. 948, 982
- Van Wagner, C. E.: Equilibrium moisture contents of some fine forest fuels in eastern Canada, Information Report, Petawawa Forest Experiment Station, 1972. 942
- Van Wagner, C. E. and Pickett, T. L.: Equations and FORTRAN program for the Canadian  
20 forest fire weather index system, in: Canadian Forestry Service, Petawawa national forestry institute, Chalk River, Ontario, Vol. 33, 1985. 941
- Venevsky, S., Thonicke, K., Sitch, S., and Cramer, W.: Simulating fire regimes in human-dominated ecosystems: Iberian Peninsula case study, *Glob. Change Biol.*, 8, 984–998, doi:10.1046/j.1365-2486.2002.00528.x, 2002. 936
- 25 Viedma, O., Meliá, J., Segarra, D., and García-Haro, J.: Modeling rates of ecosystem recovery after fires by using landsat TM data, *Remote Sens.*, 61, 383–398, 1997. 948
- Viney, N.: A review of fine fuel moisture modelling, *Int. J. Wildland Fire*, 1, 215–234, doi:10.1071/WF9910215, 1991. 941, 942
- 30 Vivian, L. M., Cary, G. J., Bradstock, R. A., and Gill, A. M.: Influence of fire severity on the regeneration, recruitment and distribution of eucalypts in the Cotter River Catchment, Australian Capital Territory, *Aust. Ecol.*, 33, 55–67, doi:10.1111/j.1442-9993.2007.01790.x, 2008. 978
- Weedon, J. T., Cornwell, W. K., Cornelissen, J. H. C., Zanne, A. E., Wirth, C., and Coomes, D. A.: Global meta-analysis of wood decomposition rates: a role for trait variation

## Parameterisation of fire in LPX1 vegetation model

D. I. Kelley et al.

[Title Page](#)

[Abstract](#)

[Introduction](#)

[Conclusions](#)

[References](#)

[Tables](#)

[Figures](#)

◀

▶

◀

▶

[Back](#)

[Close](#)

[Full Screen / Esc](#)

[Printer-friendly Version](#)

[Interactive Discussion](#)



among tree species?, *Ecol. Lett.*, 12, 45–56, doi:10.1111/j.1461-0248.2008.01259.x, 2009.  
943

Williams, P. R.: Fire-stimulated rainforest seedling recruitment and vegetative regeneration in  
5 a densely grassed wet sclerophyll forest of north-eastern Australia, *Aust. J. Bot.*, 48, 651–  
658, 2000. 945, 948

Williams, R. J., Griffiths, A. D., and Allan, G.: Fire regimes and biodiversity in the wet-dry  
tropical savanna landscapes of northern Australia, in: *Flammable Australia: Fire Regimes*  
and *Biodiversity of a Continent*, edited by: Bradstock, R., Williams, J. A., and Gill, A., 281–  
304, Cambridge University Press, Cambridge, 2002. 933

10 Xiao, J. and Moody, A.: A comparison of methods for estimating fractional green vegetation  
cover within a desert-to-upland transition zone in central New Mexico, USA, *Remote Sens.  
Environ.*, 98, 237–250, doi:10.1016/j.rse.2005.07.011, 2005. 954

Zammit, C. and Westoby, M.: Seedling recruitment strategies in obligate-seeding and resprouting  
Banksia shrubs, *Ecology*, 1984–1992, 1987. 950

---

Parameterisation of  
fire in LPX1  
vegetation model

D. I. Kelley et al.

---

Title Page

Abstract

Introduction

Conclusions

References

Tables

Figures



◀

▶



Full Screen / Esc

Printer-friendly Version

Interactive Discussion



## Parameterisation of fire in LPX1 vegetation model

D. I. Kelley et al.

[Title Page](#)

[Abstract](#)

[Introduction](#)

[Conclusions](#)

[References](#)

[Tables](#)

[Figures](#)

◀

▶

◀

▶

[Back](#)

[Close](#)

[Full Screen / Esc](#)

[Printer-friendly Version](#)

[Interactive Discussion](#)



**Table 1.** Plant functional type (PFT)-specific values used in LPX-Mv1. TBE denotes tropical broadleaf evergreen tree, TBD denotes tropical broadleaf deciduous tree, tBE denotes temperate broadleaf evergreen tree, and tBD temperate broadleaf deciduous tree. Values for resprouting variants (RS) of each of these PFTs are given in brackets. If no resprouting value is given then the resprouting PFT takes the normal PFT value. tNE denotes temperate needleleaf evergreen; BNE denotes boreal needleleaf evergreen; BBD denotes boreal broadleaf deciduous; C<sub>3</sub>: C<sub>3</sub> grass; C<sub>4</sub> grass. BT par<sub>i</sub> is the bark thickness parameter used in Eqs. (25) and (26); k<sub>10,leaf</sub> and k<sub>10,wood</sub> are the reference litter decomposition rates of leaf and grass used in Eq. (2); Q<sub>10</sub> is the parameter describing woody litter decomposition rate changes with temperature in Eq. (21).

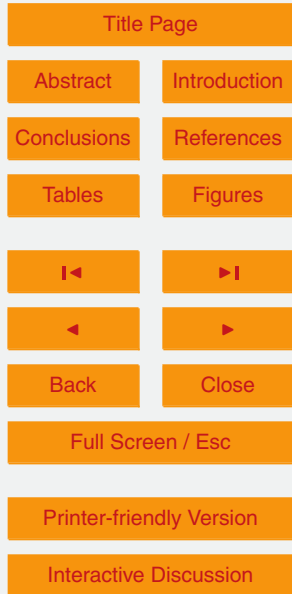
	TBE	TBD	tNE	tBE	tBD	BNE	BBD	C <sub>3</sub>	C <sub>4</sub>
fraction of roots in upper soil layer	0.80	0.70	0.85	0.80	0.80	0.85	0.80	0.90	0.85
BT par <sub>lower</sub>	0.00395 (0.0292)	0.00463 (0.0109)	0.00609 (0.0286)	0.0125 (0.0106)	0.00617 (0.0106)	0.0158	0.00875	N/A	N/A
BT par <sub>mid0</sub>	0.0167 (0.0629)	0.0194 (0.0568)	0.0257 (0.0586)	0.0302 (0.0343)	0.0230 (0.0343)	0.0261	0.0316	N/A	N/A
BT par <sub>upper</sub>	0.0399 (0.183)	0.0571 (0.188)	0.0576 (0.156)	0.0909 (0.106)	0.0559 (0.106)	0.0529	0.112	N/A	N/A
k <sub>10,leaf</sub>	0.93	1.17	0.70	0.86	0.95	0.78	0.94	1.20	0.97
k <sub>10,wood</sub>	0.039	0.039	0.041	0.104	0.104	0.041	0.104	N/A	N/A
Q <sub>10</sub>	2.75	2.75	1.97	1.37	1.37	1.97	1.37	N/A	N/A

## Parameterisation of fire in LPX1 vegetation model

D. I. Kelley et al.

**Table 2.** Translation between LPX Plant Functional Types (PFTs) and the vegetation trait information available for sites which were used to provide rooting depths.

LPX PFT	Rooting depth vegetation type from Fig. 3	Site information			
		Site leaf type	Site Phenology	Site Climate	Site Life form
TBE tBE	Evergreen Broadleaf	Broad only	Evergreen	Any	Tree only
TBD	Drought Deciduous Broadleaf	Broad only	Drought deciduous	Any	Tree only
tBD BBB	Cold Deciduous Broadleaf	Broad only	Cold/Winter deciduous	Any	Tree only
TN BN	Needle-leaf	Needle only	Any	Any	Tree only Tree only
C <sub>3</sub> Grass	Cold grassland	Any	Any	MTCO $\leq$ 15.5 °C	Grass or Herb
C <sub>4</sub> Grass	Warm grassland	Any	Any	MTCO > 15.5 °C	Grass or Herb



## Parameterisation of fire in LPX1 vegetation model

D. I. Kelley et al.

[Title Page](#)

[Abstract](#)

[Introduction](#)

[Conclusions](#)

[References](#)

[Tables](#)

[Figures](#)

◀

▶

[Back](#)

[Close](#)

[Full Screen / Esc](#)

[Printer-friendly Version](#)

[Interactive Discussion](#)



**Table 3.** Summary of studies on post-fire recruitment rates used to derive a recruitment penalty for resprouting PFTs in LPX-Mv1. All of the study sites contained resprouting (RS) and non-resprouting (NR) species.

Reference	Measure	Species	Values	Implied recruitment penalty
Vivian et al. (2008)	Ratio of seedlings to pre-basal fire area	<i>Eucalyptus fastigata</i> (RS)	0.05	86 %
		<i>E. delegatensis</i> (NR)	0.35	
Silva-Matos et al. (2005)	Number of seedlings 3 months after fire	<i>Cecropia</i> (RS)	1	100 %
		<i>Trema</i> (NR)	405	
Enright and Goldblum (1999)	Post-fire recruitment and seedling survival	<i>Hakea rostrata</i> (RS)	NS 10× greater recruitment, 7× greater survival	85–90 %
		<i>H. decurrens</i> (NR)		
Biganzoli et al. (2009)	Post-fire seedling recruitment	<i>Eupatorium buniifolium</i> (RS)	<i>E. buniifolium</i> recruitment	96 %
		<i>Baccharis dracunculifolia</i> (NR)	6 % of <i>B. dracunculifolia</i>	
Enright and Lamont (1989)	Seedling per parent, after fire	<i>Banksia attenuata</i> (RS)	5.1, 14.6	93 %
		<i>B. menziesii</i> (RS)	1.1, 1.0	
		<i>B. candolleana</i> (RS)	0.5, 3.2	
		<i>B. hookeriana</i> (NR)	37.3, 73.5	
		<i>B. leptophylla</i> (NR)	185.6, 95.0	

## Parameterisation of fire in LPX1 vegetation model

D. I. Kelley et al.

[Title Page](#)[Abstract](#)[Introduction](#)[Conclusions](#)[References](#)[Tables](#)[Figures](#)[◀](#)[▶](#)[◀](#)[▶](#)[Back](#)[Close](#)[Full Screen / Esc](#)[Printer-friendly Version](#)[Interactive Discussion](#)

---

**Parameterisation of fire in LPX1 vegetation model**

D. I. Kelley et al.

**Table 5.** Information used to calculate recovery time at sites with different fire-response adaptations. The dominant fire responses (Dominant adaptation) are AR: aerial resprouters (RS), BR: basal RS, OS: obligate seeder, and R: RS of unknown type. NR indicates vegetation with no specific fire adaptation. AR and BR sites are used to represent RS in Fig. 7, while UR, R and OS are grouped together as OS in Fig. 7. Med stands for Mediterranean-type climate. The proportion decrease (%) in the vegetation index of a site after fire is given in Impact. The vegetation indices are NDVI: Normalised Difference Vegetation Index, NDVI anomalies: the deviation of NDVI from the expected value; EVI: the Enhanced vegetation index; or a site-specific index as described in the original publication. The impact of fire was expressed either with respect to local sites that were not burnt (control) or to pre-fire values at the burnt site (pre-fire), or to the maximum value found in pre-fire years (maximum). The time to recovery is the length of time required before the Veg Index reaches 90 % of the pre-fire cover. Where this is based on an extrapolation beyond the years of observation, the number of extrapolated years is given (Extrapolated Years).

<a href="#">Title Page</a>	
<a href="#">Abstract</a>	<a href="#">Introduction</a>
<a href="#">Conclusions</a>	<a href="#">References</a>
<a href="#">Tables</a>	<a href="#">Figures</a>
<a href="#">◀</a>	<a href="#">▶</a>
<a href="#">◀</a>	<a href="#">▶</a>
<a href="#">Back</a>	<a href="#">Close</a>
<a href="#">Full Screen / Esc</a>	
<a href="#">Printer-friendly Version</a>	
<a href="#">Interactive Discussion</a>	

## Parameterisation of fire in LPX1 vegetation model

D. I. Kelley et al.

[Title Page](#)

[Abstract](#)

[Introduction](#)

[Conclusions](#)

[References](#)

[Tables](#)

[Figures](#)



[Full Screen / Esc](#)

[Printer-friendly Version](#)

[Interactive Discussion](#)



**Table 5.** Continued.

Dominant Adaptation	Dominant Species	Climate	Impact (%)	Veg Index	Comparison	Interpolate to recovery (yr)	Time to recovery (yr months)	Reference
RS in Fig. 7								
AR	<i>Quercus suber</i>	Med	47	NDVI	control	6	13 yr 6 m	Diaz-Delgado et al. (1998)
	<i>Quercus suber</i>	Med	44	NDVI	control	0	5 yr 2 m	Diaz-Delgado et al. (1998)
	<i>Quercus suber</i>	Med	78	NDVI	control	0	7 yr 3 m	Díaz-Delgado et al. (2002)
	<i>Eucalyptus</i> sp.	Med	27	NDVI	Gorgeous years	8	10 yr 2 m	Gouveia et al. (2010)
	<i>Quercus agrifolia</i>	Med	69	NDVI	pre-fire	0	4 yr 4 m	Hope et al. (2007)
AR/BR	<i>Adenostoma fasciculatum</i> ; <i>Ceanothus</i> sp.; <i>Aristostaphylos</i> sp.; <i>Quercus dumosa</i> ; <i>Rhus ovata</i> ; <i>Heteromeles arbutifolia</i>	Med	58	NDVI	control	7	8 yr 3 m	Riaño et al. (2002)
	coastal sage scrub	Med	43	NDVI	control	0	0 yr 2 m	Riaño et al. (2002)
	<i>Arctostaphylos glauca</i> ; <i>Ceanothus megacarpus</i> ; <i>Cercocarpus betuloides</i> ; <i>Rhamnus ilicifolia</i> ; <i>Eriogonum fasciculatum</i> ; <i>Ceanothus thyrsiflorus</i> ; <i>Adenostoma fasciculatum</i> ; <i>Ceanothus greggii</i> ; <i>Arctostaphylos glandulosa</i> ; <i>Ceanothus crassifolius</i> ; <i>Ceanothus cuneatus</i> ; <i>Ceanothus leucodermis</i> ; <i>Prunus ilicifolia</i> ssp. <i>ilicifolia</i>	Med	72	NDVI	pre-fire	0	5 yr 10 m	Hope et al. (2007)
AR/BR	<i>Arctostaphylos glauca</i> ; <i>Ceanothus megacarpus</i> ; <i>Cercocarpus betuloides</i> ; <i>Rhamnus ilicifolia</i> ; <i>Eriogonum fasciculatum</i> ; <i>Ceanothus thyrsiflorus</i> ; <i>Adenostoma fasciculatum</i> ; <i>Ceanothus greggii</i> ; <i>Arctostaphylos glandulosa</i> ; <i>Ceanothus crassifolius</i> ; <i>Ceanothus cuneatus</i> ; <i>Ceanothus leucodermis</i> ; <i>Prunus ilicifolia</i> ssp. <i>ilicifolia</i>	Med	60	NDVI	pre-fire	0	4 yr 10 m	Hope et al. (2007)
BR	<i>Salvia apiana</i> ; <i>Salvia leucophylla</i> ; <i>Salvia mellifera</i> ; <i>Artemisia californica</i> ; <i>Eriogonum cinereum</i> ; <i>Eriogonum elongatum</i> ; <i>Eriogonum fasciculatum</i> ; <i>Encelia californica</i> ; <i>Lotus</i> ; <i>Lupinus</i> ; <i>Mimulus</i>	Med	33	NDVI	control	6	10 yr 0 m	Riaño et al. (2002)
	<i>Salvia apiana</i> ; <i>Salvia leucophylla</i> ; <i>Salvia mellifera</i> ; <i>Artemisia californica</i> ; <i>Eriogonum cinereum</i> ; <i>Eriogonum elongatum</i> ; <i>Eriogonum fasciculatum</i> ; <i>Encelia californica</i> ; <i>Lotus</i> ; <i>Lupinus</i> ; <i>Mimulus</i>	Med	48	NDVI	control	8	11 yr 7 m	Riaño et al. (2002)
	<i>Quercus ilex</i> ; <i>Pinus halepensis</i>	Med	46	NDVI	control	6	14 yr 5 m	Diaz-Delgado et al. (1998)
	<i>Adenostoma fasciculatum</i> ; <i>Salvia mellifera</i> ; <i>Salvia apiana</i>	Med	70	NDVI	pre-fire	0	5 yr 10 m	Hope et al. (2007)
	<i>Eriogonum fasciculatum</i> ; <i>Salvia apiana</i>	Med	67	NDVI	pre-fire	0	7 yr 2 m	Hope et al. (2007)

## Parameterisation of fire in LPX1 vegetation model

D. I. Kelley et al.

**Table 5.** Continued.

Dominant Adaptation	Dominant Species	Climate	Impact (%)	Veg Index	Comparison	Interpolate to recovery (yr)	Time to recovery (yr months)	Reference
OS in Fig. 7								
R/OS	Pinus ponderosa; Quercus gambelii; Pinus edulis		81	EVI	Pre-fire	5	9 yr 6 m	Casady et al. (2009)
OS	<i>Pinus halepensis</i> ; <i>Rosmarinus officinalis</i> ; <i>Erica multiflora</i> ; <i>Ulex parviflorus</i> ; <i>Brachypodium retusum</i>	dry – subhumid Med	15	NDVI	control	8	15 yr 9 m	van Leeuwen et al. (2010)
	<i>Quercus ilex</i> ; <i>Pinus halepensis</i> ; Shrubland	Med	91	NDVI	control	6	8 yr 6 m	Díaz-Delgado et al. (2003)
	<i>Pinus pinaster</i>	Med	31	NDVI	Gorgeous years	8	10 yr 1 m	Gouveia et al. (2010)
	<i>Pinus pinaster</i>	Med	63	Own index	Index	6	13y11m	Solans Vila and Barbosa (2010)
NR	<i>Pinus ponderosa</i> needle-leaf evergreen species	Boreal	63	NDVI anomalies	control	7 0	12 yr 0 m 6yr 6 m	van Leeuwen (2008) Goetz et al. (2006)
	needle-leaf evergreen species	Boreal	36	NDVI anomalies	control	8	15 yr 1 m	Goetz et al. (2006)
	needle-leaf evergreen species	Boreal	43	NDVI	control	6	21 yr 11 m	Epting and Verbyla (2005)
	evergreen needle-leaf forest	Boreal	18	NDVI	control	8	20 yr 7 m	Cuevas-González et al. (2009)
	deciduous needle-leaf forest	Boreal	22	NDVI	control	7	20 yr 0 m	Cuevas-González et al. (2009)

[Title Page](#)

[Abstract](#)

[Introduction](#)

[Conclusions](#)

[References](#)

[Tables](#)

[Figures](#)

◀

▶

◀

▶

[Back](#)

[Close](#)

[Full Screen / Esc](#)

[Printer-friendly Version](#)

[Interactive Discussion](#)



## Parameterisation of fire in LPX1 vegetation model

D. I. Kelley et al.

[Title Page](#)

[Abstract](#)

[Introduction](#)

[Conclusions](#)

[References](#)

[Tables](#)

[Figures](#)



[Back](#)

[Close](#)

[Full Screen / Esc](#)

[Printer-friendly Version](#)

[Interactive Discussion](#)



**Table 6.** Scores obtained using the mean of the data (Data mean), and the mean and standard deviation of the scores obtained from bootstrapping experiments (Bootstrap mean, Bootstrap SD). Step 1 is a straight comparison; 2 is a comparison with the influence of the mean removed; 3 is with mean and variance removed. The scores given for fire represent the range of scores over all fire datasets for that comparison. Scores for individual datasets can be found in Table S1.

Variable	Step	Measure	Time period	Mean	Bootstrap mean	Bootstrap SD
Fire: All Aus	1	Annual average	1997–2006	1.00	1.14–1.25	0.0028–0.015
	2			1.00	1.18–1.26	0.0037–0.010
	3			1.00	1.20–1.30	0.0053–0.016
	2	IAV		1.00	1.31–1.50	0.34–0.36
	1	Seasonal Concentration		1.00	1.32–1.36	0.0073–0.020
	N/A	Phase		0.39–0.45	0.44–0.47	0.0015–0.0046
	1	Annual average		1.00	1.13–1.20	0.024–0.0256
	2			1.00	1.18–1.20	0.024–0.0257
	3			1.00	1.20–1.21	0.024–0.025
	2	IAV		1.00	1.24–1.32	0.33–0.37
Fire: SE Aus	1	Seasonal Concentration		1.00	1.31–1.33	0.043–0.053
	N/A	Phase		0.44–0.47	0.47	0.010–0.011
	N/A	life forms	1992–1993	0.71	0.89	0.0018
	N/A	tree cover		0.43	0.54	0.0015
	N/A	herb cover		0.49	0.66	0.0017
	N/A	bare ground		0.46	0.56	0.0017
	N/A	broadleaf		0.83	0.96	0.0041
	N/A	evergreen		0.70	0.87	0.0032
fine litter NPP	1	Annual average	1997–2005	1.00	1.44	0.21
	2			1.00	1.44	0.22
	3			1.00	1.43	0.095
	1	Annual average		1.00	1.33	0.015
	2			1.00	1.33	0.015
fAPAR	3			1.00	1.32	0.014
	2	IAV		1.00	1.23	0.32
	3			1.00	1.35	0.36
	1	Seasonal Conc		1.00	1.46	0.014
	2			1.00	1.46	0.014
	3			1.00	1.45	0.014
	N/A	Phase		0.30	0.38	0.0033
	1	Annual average	2005	1.00	1.32	0.016
	2			1.00	1.32	0.016
	3			1.00	1.31	0.016

## Parameterisation of fire in LPX1 vegetation model

D. I. Kelley et al.

[Title Page](#)

[Abstract](#)

[Introduction](#)

[Conclusions](#)

[References](#)

[Tables](#)

[Figures](#)

◀

▶

◀

▶

[Back](#)

[Close](#)

[Full Screen / Esc](#)

[Printer-friendly Version](#)

[Interactive Discussion](#)



## Parameterisation of fire in LPX1 vegetation model

D. I. Kelley et al.

[Title Page](#)[Abstract](#)[Introduction](#)[Conclusions](#)[References](#)[Tables](#)[Figures](#)[Back](#)[Close](#)[Full Screen / Esc](#)[Printer-friendly Version](#)[Interactive Discussion](#)**Table 7.** Continued.

Variable	Metric	Measure	LPX	Lightn	Drying	Roots	Litter	Bark	LPX-M v1-nr	LPX-M v1-rs
burnt area: SE Aus	Mean	Annual Average	0.048	0.099	0.053	0.051	0.012	0.002	0.024	0.024
	Mean ratio		6.00–10.9	12.4–22.6	6.68–12.2	6.37–11.6	1.55–2.83	0.25–0.49	3.07–6.61	2.98–5.42
	NME S1	Annual Average	4.03–7.19	7.97–14	4.35–7.67	4.23–7.59	<b>1.59–2.40</b>	0.81*–0.92*	<b>2.29–4.27</b>	<b>2.33–3.67</b>
	NME S2		3.58–6.13	5.07–7.91	<b>3.6–6.06</b>	3.61–6.21	<b>1.78–2.99</b>	<b>1.05*–1.08*</b>	<b>2.50–4.75</b>	<b>2.53–4.20</b>
	NME S3		1.33–2.07	<b>1.28–1.34</b>	<b>1.32–1.37</b>	<b>1.32–1.40</b>	<b>1.22–1.25</b>	<b>1.18*–1.22</b>	<b>1.26–1.29</b>	<b>1.26–1.30</b>
	NME S2	Inter-annual variability	8.59–16.6	10.1–19.3	9.05–17.5	10.1–19.4	<b>3.83–7.65</b>	<b>1.27–2.33</b>	<b>5.56–11.5</b>	5.71–11.2
Veg cover	Mean	Trees	0.034	0.011	0.022	0.034	0.059	0.075	0.042	0.049
	Mean ratio		0.4	0.13	0.26	0.4	0.69	0.88	0.49	0.58
	Mean	Herb	0.44	0.34	0.45	0.44	0.55	0.57	0.55	0.55
	Mean ratio		0.65	0.5	0.65	0.65	0.81	0.84	0.80	0.81
	Mean	Bare ground	0.52	0.65	0.53	0.52	0.39	0.35	0.41	0.4
	Mean ratio		2.79	3.45	2.83	2.77	2.08	1.88	2.18	2.12
	Mean	Phenology	0.066	0.014	0.042	0.063	0.12	0.15	0.10	0.12
	Mean ratio		0.13	0.026	0.081	0.12	0.23	0.28	0.20	0.22
	Mean	Leaf type	0.055	0.01	0.035	0.056	0.1	0.14	0.096	0.11
	Mean ratio		0.094	0.018	0.059	0.096	0.18	0.24	0.17	0.18
Veg Cover	MM	Life Form	<b>0.77*</b>	0.96	<b>0.79*</b>	<b>0.76*</b>	<b>0.59*</b>	<b>0.56*</b>	<b>0.59*</b>	<b>0.58*</b>
		Trees	<b>0.16*</b>	<b>0.17*</b>	<b>0.17*</b>	<b>0.17*</b>	<b>0.19*</b>	<b>0.17*</b>	<b>0.17*</b>	<b>0.16*</b>
		Herb	0.66	0.77	0.67	<b>0.65*</b>	<b>0.53*</b>	<b>0.52*</b>	<b>0.51*</b>	<b>0.51*</b>
		Bare ground	0.72	0.95	0.73	<b>0.71</b>	<b>0.49*</b>	<b>0.42*</b>	<b>0.51*</b>	<b>0.49*</b>
		Phenology	<b>0.29*</b>	<b>0.33*</b>	<b>0.24*</b>	<b>0.29*</b>	<b>0.61*</b>	<b>0.81*</b>	0.72	0.46
		Leaf type	<b>0.51*</b>	1.01	<b>0.62*</b>	<b>0.46*</b>	<b>0.34*</b>	<b>0.27*</b>	<b>0.15*</b>	<b>0.19*</b>
Fine NPP	Mean	Annual Average	628	112	192	180	177	176	181	202
	Mean ratio		2.67	0.5	0.85	0.8	0.78	0.80	0.82	0.90
	NME S1		2.62	<b>0.96*</b>	<b>0.79*</b>	<b>0.78*</b>	<b>0.82*</b>	<b>1.13*</b>	<b>0.80*</b>	<b>0.73*</b>
	NME S2		1.47	<b>0.83*</b>	<b>0.79*</b>	<b>0.78*</b>	<b>0.83*</b>	<b>1.22*</b>	<b>0.79*</b>	<b>0.74*</b>
	NME S3		0.97*	<b>0.91*</b>	1.01*	<b>0.89*</b>	1.01*	2.00	0.99*	<b>0.87*</b>
fAPAR	Mean	Annual Average	0.19	0.12	0.19	0.18	0.24	0.26	0.22	0.22
	Mean ratio		1.59	1.02	1.56	1.55	2.02	2.18	1.83	1.87
	NME S1	Annual Average	1.11*	<b>0.98*</b>	1.11*	<b>1.07*</b>	1.61	1.8	1.31	1.35
	NME S2		0.69*	<b>0.97*</b>	0.72*	<b>0.68*</b>	0.7*	<b>0.69*</b>	<b>0.61*</b>	<b>0.61*</b>
	NME S3		0.71*	1.21*	0.76*	0.71*	<b>0.57*</b>	<b>0.51*</b>	<b>0.57*</b>	<b>0.54*</b>
	NME S2	Inter-annual variability	1.01	1.11	1.01	<b>0.97</b>	2.44	2.86	1.83	1.85
	NME S3	Seasonal Conc.	1.34*	1.44	1.35*	1.36*	<b>1.31*</b>	<b>1.31*</b>	<b>1.32*</b>	<b>1.33*</b>
	MPD	Phase	0.25*	0.25*	0.25*	<b>0.24*</b>	0.25*	0.25*	<b>0.24*</b>	<b>0.24*</b>
height	Mean	Annual Average	0.5	0.2	0.29	0.5	0.84	1.03	0.39	0.63
	Mean ratio		0.056	0.022	0.033	0.057	0.096	0.12	0.045	0.072
	NME S1		1.07*	1.1*	1.09*	1.07*	<b>1.02*</b>	<b>1.01*</b>	1.08*	<b>1.05*</b>
	NME S2		0.94*	<b>0.98*</b>	0.97*	0.94*	<b>0.91*</b>	<b>0.9*</b>	<b>0.96*</b>	<b>0.94*</b>
	NME S3		1.25*	1.39	1.31*	1.26*	1.11*	<b>1.08*</b>	1.18*	1.13*

**Table A1.** Allocation of species to plant functional type (PFT) and to aerial resprouting (RS) and non-resprouting (NR) and other resprouting/unknown resprouting type (other) categories for the bark thickness analyses. All species listed (RS, NR and other) for each PFT were used for the parametrisation of bark thickness (BT) in LPX-Mv1-nr; RS species were used to parameterise BT for LPX-Mv1-rs RS PFTs; and NR for LPX-Mv1-rs NR PFTs.

PFT	Type	Species
TBE	RS	<i>Acacia lamprocarpa</i> , <i>Alstonia actinophylla</i> , <i>Banksia</i> sp., <i>B. dentata</i> , <i>Corymbia bella</i> , <i>Eucalyptus miniata</i> , <i>E. phoenicea</i> , <i>E. tectifica</i> , <i>E. tetrodonta</i> , <i>Gardenia megasperma</i> , <i>Lophostemon lactifluous</i> , <i>Melaleuca</i> , <i>M. nervosa</i> , <i>M. viridiflora</i> , <i>Persoonia falcata</i> , <i>Syzygium eucalyptoides</i> subsp. <i>bleeseri</i> , <i>S. suborbicularis</i> , <i>Xanthostemon paradoxus</i>
NR		<i>Abarema jupunba</i> , <i>A. mataybifolia</i> , <i>Acacia auriculiformis</i> , <i>Agonandra silvatica</i> , <i>Aiouea longipetiolata</i> , <i>Alexa wachenheimii</i> , <i>Amaioua corymbosa</i> , <i>A. guianensis</i> , <i>Ambellaria acida</i> , <i>Amblygonocarpus obtusangulus</i> , <i>Amburara cearensis</i> , <i>Amherstia nobilis</i> , <i>Amphirrhox longifolia</i> , <i>Anacardium spruceanum</i> , <i>Anartia meyeri</i> , <i>Aniba guianensis</i> , <i>A. hostmanniana</i> , <i>A. panurensis</i> , <i>A. terminalis</i> , <i>A. williamsii</i> , <i>Annona prevostiae</i> , <i>Antonia ovata</i> , <i>Arachidendron kunstleri</i> , <i>Aspidosperma album</i> , <i>A. cruentum</i> , <i>A. marcgravianum</i> , <i>A. oblongum</i> , <i>A. spruceanum</i> , <i>Astronium lecoitae</i> , <i>A. ulei</i> , <i>Bagassa guianensis</i> , <i>Baikiaea insignis</i> subsp. <i>minor</i> , <i>Balizia pedicellaris</i> , <i>Bauhinia aculeata</i> , <i>B. blakeana</i> , <i>B. monandra</i> , <i>B. tomentosa</i> , <i>Bocca alterna</i> , <i>B. prouacensis</i> , <i>Bonafousia undulata</i> , <i>Brosimum guineense</i> , <i>B. rubescens</i> , <i>B. utile</i> , <i>Brownea ariza</i> , <i>B. latifolia</i> , <i>Buchenavia</i> sp., <i>B. grandis</i> , <i>B. guianensis</i> , <i>B. tetraphylla</i> , <i>Bunchosia</i> sp., <i>Caesalpinia calycina</i> , <i>C. echinata</i> , <i>C. ferrea</i> , <i>C. nicaraguensis</i> , <i>C. pluviosa</i> , <i>C. pulcherrima</i> , <i>C. sappan</i> , <i>C. vesicaria</i> , <i>Callandria sancti-pauli</i> , <i>Calyptranthes speciosa</i> , <i>Capirona decorticans</i> , <i>Carapa procera</i> , <i>Casearia</i> sp., <i>C. decandra</i> , <i>C. javitensis</i> , <i>C. sylvestris</i> , <i>Cassipourea guianensis</i> , <i>Castanospermum australe</i> , <i>Cathedra acuminata</i> , <i>Catostemma fragrans</i> , <i>Cecropia obtusa</i> , <i>Chaetocarpus</i> sp., <i>C. schomburgkiana</i> , <i>Chaunochnothrix kappleri</i> , <i>Cheiloclinium cognatum</i> , <i>Chimarrhis turbinata</i> , <i>Chloroleucon mangense</i> , <i>Coccobola mollis</i> , <i>Cojoba filicifolia</i> , <i>Conceveiba guianensis</i> , <i>Couratari calycina</i> , <i>C. gloriae</i> , <i>C. guianensis</i> , <i>C. multiflora</i> , <i>C. oblongifolia</i> , <i>Crepidospermum goudotianum</i> , <i>Cupania diphylla</i> , <i>C. rubiginosa</i> , <i>C. scrobiculata</i> , <i>C. scrobiculata</i> var. <i>guianensis</i> , <i>Cupaniopsis anacardioides</i> , <i>Cyrilliosis paraisensis</i> , <i>Dacryodes cuspidata</i> , <i>D. nitens</i> , <i>Daubergia ferruginea</i> , <i>D. frutescens</i> , <i>D. glandulosa</i> , <i>D. monetaria</i> , <i>D. nigra</i> , <i>D. polyphylla</i> , <i>D. riparia</i> , <i>D. villosa</i> , <i>Dendrobangia boliviiana</i> , <i>Dicorynia guianensis</i> , <i>Diospyros calycintha</i> , <i>D. capreifolia</i> , <i>D. carbonaria</i> , <i>D. cavalcantei</i> , <i>D. dichroa</i> , <i>Diplotropis purpurea</i> , <i>D. brachypetala</i> , <i>Dipteryx odorata</i> , <i>D. punctata</i> , <i>Discophora guianensis</i> , <i>Drypetes deplochelei</i> , <i>Dugueta calycina</i> , <i>D. surinamensis</i> , <i>Dulacia guianensis</i> , <i>Duroia aquatica</i> , <i>D. eriopila</i> , <i>D. longiflora</i> , <i>Ecclinusa lanceolata</i> , <i>E. ramiflora</i> , <i>Ecuadendron acosta-solisianum</i> , <i>Elaeoluma</i> sp., <i>E. nuda</i> , <i>Ermatomutus flagifolium</i> , <i>Endlicheria mellionii</i> , <i>Enterolobium schomburgkii</i> , <i>Eperua falcatia</i> , <i>E. grandiflora</i> , <i>Erisma floribundum</i> , <i>E. uncinatum</i> , <i>Eschweilera apiculata</i> , <i>E. chartacea</i> , <i>E. congestiflora</i> , <i>E. coriacea</i> , <i>E. decorans</i> , <i>E. grandiflora</i> , <i>E. micrantha</i> , <i>E. parviflora</i> , <i>E. pedicellata</i> , <i>E. praeclara</i> , <i>E. sagotiana</i> , <i>E. simiorum</i> , <i>E. squamata</i> , <i>Eugenia</i> sp., <i>E. coffeefolia</i> , <i>E. cucullata</i> , <i>E. cupulata</i> , <i>E. macrocalyx</i> , <i>E. patrisii</i> , <i>E. pseudosipidium</i> , <i>E. tapacumensis</i> , <i>E. tetrameria</i> , <i>Euterpe oleracea</i> , <i>Exelloidendron barbatum</i> , <i>Exocorpus latifolius</i> , <i>Faramea pendulculata</i> , <i>Ferdinandusa paraensis</i> , <i>Fusaea longifolia</i> , <i>Geissospermum laeve</i> , <i>Grevillea</i> sp., <i>G. pteridifolia</i> , <i>G. costata</i> , <i>G. grandifolia</i> , <i>G. guidonia</i> , <i>G. scabra</i> , <i>G. silvatica</i> , <i>Guatteria anthracina</i> , <i>G. guianensis</i> , <i>G. wachenheimii</i> , <i>Guibourtia copallifera</i> , <i>Gustavia hexapetala</i> , <i>Haematoxylum campechianum</i> , <i>H. campeşianum</i> , <i>Hebepepetalum humifusifolium</i> , <i>Heisteria densifrons</i> , <i>Helicostylis pedunculata</i> , <i>H. tomentosa</i> , <i>Henriettaea flavescentia</i> , <i>Hevea guianensis</i> , <i>Holocalyx glaziovii</i> , <i>Hortia excelsa</i> , <i>Humiriastylum subcrenatum</i> , <i>Hyperinoma alchorneoides</i> , <i>Ilex arrhemensis</i> , <i>Inga</i> sp., <i>I. acarea</i> , <i>I. acrocephala</i> , <i>I. alba</i> , <i>I. albicoria</i> , <i>I. brachystachys</i> , <i>I. calderoni</i> , <i>I. densiflora</i> , <i>I. edulis</i> , <i>I. fanchoniana</i> , <i>I. gracilifolia</i> , <i>I. huberi</i> , <i>I. leioacalycina</i> , <i>I. longipedunculata</i> , <i>I. loubryana</i> , <i>I. marginata</i> , <i>I. melinonii</i> , <i>I. nobilis</i> , <i>I. nouraquensis</i> , <i>I. nuda</i> , <i>I. oerstediana</i> , <i>I. paraensis</i> , <i>I. pezizifera</i> , <i>I. punctata</i> , <i>I. rubiginosa</i> , <i>I. sarmentosa</i> , <i>I. sessilis</i> , <i>I. spectabilis</i> , <i>I. stipularis</i> , <i>I. subnuda</i> , <i>I. tenuistipula</i> , <i>Iryanthera hostmannii</i> , <i>I. sagotiana</i> , <i>Jessenia bataua</i> , <i>Lacistema grandifolium</i> , <i>Lacistema aculeata</i> , <i>Lacunaria crenata</i> , <i>L. jenmanii</i> , <i>Lecythis chartacea</i> , <i>L. corrugata</i> , <i>L. hologyne</i> , <i>L. idatimon</i> , <i>L. persistsens</i> , <i>L. poiteaui</i> , <i>L. zabucajo</i> , <i>Leonia glycycarpa</i> , <i>Licania</i> sp., <i>L. alba</i> , <i>L. canescens</i> , <i>L. glaberriflora</i> , <i>L. heteromorpha</i> , <i>L. kunthiana</i> , <i>L. laevigata</i> , <i>L. latistipula</i> , <i>L. laxiflora</i> , <i>L. licaniflora</i> , <i>L. majuscula</i> , <i>L. membranacea</i> , <i>L. micrantha</i> , <i>L. minutiflora</i> , <i>L. octandra</i> , <i>L. ovalifolia</i> , <i>L. sprucei</i> , <i>Licaria cannela</i> , <i>L. chrysophylla</i> , <i>L. guianensis</i> , <i>Loreya arborescens</i> , <i>Lueheopsis rugosa</i> , <i>Mabea</i> sp., <i>M. piriri</i> , <i>M. speciosa</i> , <i>Machaerium acaciaefolium</i> , <i>M. inundatum</i> , <i>M. stipitatum</i> , <i>Mallacouba guianensis</i> , <i>Mallotus philippensis</i> , <i>Malouetia guianensis</i> , <i>Manilkara bidentata</i> , <i>M. huberi</i> , <i>Maprounea guianensis</i> , <i>Maquia calophylla</i> , <i>M. guianensis</i> , <i>Maytenus guyanensis</i> , <i>M. myrsinoides</i> , <i>M. oblongata</i> , <i>Melicoccus pedicellaris</i> , <i>Mezoneuron hildebrandtii</i> , <i>Miconia</i> sp., <i>M. acuminata</i> , <i>M. chartacea</i> , <i>M. cuspidata</i> , <i>M. fragilis</i> , <i>M. punctata</i> , <i>M. tschudyioides</i> , <i>Micropholis</i> sp., <i>M. cayennensis</i> , <i>M. egensis</i> , <i>M. guyanensis</i> , <i>M. longipedicellata</i> , <i>M. melinoniana</i> , <i>M. mensalis</i> , <i>M. obscura</i> , <i>M. porphyrocarpa</i> , <i>M. sanctae-rosae</i> , <i>M. venulosa</i> , <i>Minquartia guianensis</i> , <i>Moronoeba coccinea</i> , <i>Mouriri crassifolia</i> , <i>M. huberi</i> , <i>M. sagotiana</i> , <i>Moutabea guianensis</i> , <i>Mycrsia</i> sp., <i>M. decorticans</i> , <i>M. fallax</i> , <i>Myrciaria floribunda</i> , <i>Myroxylon balsamum</i> , <i>Neea floribunda</i>

# Parameterisation of fire in LPX1 vegetation model

D. I. Kelley et al.

Title Page

## Abstract

Introduction

## Conclusion

## References

## Tables

## Figures

1

▶ |

1

Back

**Close**

Full Screen / Esc

[Printer-friendly Version](#)

## Interactive Discussion



# Parameterisation of fire in LPX1 vegetation model

D. I. Kelley et al.

PFT	Type	Species
NR		<i>Ocotea</i> sp., <i>O. amazonica</i> , <i>O. argyrophylla</i> , <i>O. cinerea</i> , <i>O. indirectinervia</i> , <i>O. percurrents</i> , <i>O. schomburgkiana</i> , <i>O. subterminalis</i> , <i>O. tomentella</i> , <i>Oenocarpus bacaba</i> , <i>Ormosia coccinea</i> , <i>O. flava</i> , <i>O. pachycarpa</i> , <i>O. stipularis</i> , <i>Osteophleum platyspermum</i> , <i>Oxandra asbeckii</i> , <i>Pachira dolichocalyx</i> , <i>Palicourea guianensis</i> , <i>Parahancornia fasciculata</i> , <i>Parkia decussata</i> , <i>P. nitida</i> , <i>P. ulei</i> , <i>Parkinsonia aculeata</i> , <i>Perebea guianensis</i> , <i>P. rubra</i> , <i>Pithecellobium pruinosum</i> , <i>P. unguis-cati</i> , <i>Platonia insignis</i> , <i>Poecilanthe effusa</i> , <i>P. parviflora</i> , <i>Pogonophora schomburgkiana</i> , <i>Polalthya australis</i> , <i>Poraqueiba guianensis</i> , <i>Posoqueria latifolia</i> , <i>Pouroura bicolor</i> , <i>P. minor</i> , <i>P. tomentosa</i> , <i>Pouteria</i> sp., <i>P. ambelanifolia</i> , <i>P. bangii</i> , <i>P. benai</i> , <i>P. bilocularis</i> , <i>P. cladantha</i> , <i>P. cuspidata</i> , <i>P. decorticans</i> , <i>P. durlandii</i> , <i>P. egregia</i> , <i>P. engleri</i> , <i>P. eugeniifolia</i> , <i>P. filipes</i> , <i>P. fimbriata</i> , <i>P. flavilatax</i> , <i>P. glomerata</i> , <i>P. gonggrijpii</i> , <i>P. grandis</i> , <i>P. guianensis</i> , <i>P. hispida</i> , <i>P. jarrensis</i> , <i>P. laevigata</i> , <i>P. macrocarpa</i> , <i>P. macrophylla</i> , <i>P. maxima</i> , <i>P. melanopoda</i> , <i>P. petiolata</i> , <i>P. putamen-ovi</i> , <i>P. reticulata</i> , <i>P. retinervis</i> , <i>P. rodriquesiana</i> , <i>P. singularis</i> , <i>P. torta</i> , <i>Pradosia</i> sp., <i>P. cochlearia</i> , <i>P. ptychandra</i> , <i>Prosopis articulata</i> , <i>P. juliflora</i> , <i>P. palmeri</i> , <i>Protium</i> sp., <i>P. apiculatum</i> , <i>P. cuneatum</i> , <i>P. decandrum</i> , <i>P. demerarensis</i> , <i>P. gallicum</i> , <i>P. giganteum</i> , <i>P. guianense</i> , <i>P. morii</i> , <i>P. opacum</i> , <i>P. pallidum</i> , <i>P. plagiocarpum</i> , <i>P. sagotianum</i> , <i>P. subserratum</i> , <i>P. tenuifolium</i> , <i>P. trifoliolatum</i> , <i>Pseudopiptadenia psilospatha</i> , <i>P. suaveolens</i> , <i>Pseudoxandra cuspidata</i> , <i>Psychotria figicemma</i> , <i>P. mapouroides</i> , <i>Pterolobium lacerasans</i> , <i>P. stellatum</i> , <i>Ptychosperma olacoides</i> , <i>Qualea</i> sp., <i>Q. rosea</i> , <i>Quararibea buckleyi</i> , <i>Q. spatulata</i> , <i>Quiina</i> sp., <i>Q. guianensis</i> , <i>Q. obovata</i> , <i>Recordroydon speciosum</i> , <i>Rhabdodendron amazonicum</i> , <i>Rheedia madruno</i> , <i>Rhodostemonodaphne grandis</i> , <i>R. kunthiana</i> , <i>R. praeculta</i> , <i>R. rufovirgata</i> , <i>Rinorea</i> sp., <i>Rollinia elliptica</i> , <i>Ruizterania albiflora</i> , <i>Sacoglottis</i> sp., <i>S. cydonioides</i> , <i>S. guianensis</i> , <i>Salacia elliptica</i> , <i>Sandwithia guianensis</i> , <i>Saraca indica</i> , <i>Schefflera decaphylla</i> , <i>S. morototoni</i> , <i>Schotia humboldtii</i> , <i>Sextonia rubra</i> , <i>Simaba cedron</i> , <i>S. morettii</i> , <i>S. polyphylla</i> , <i>Simarouba amara</i> , <i>Siparuna cristata</i> , <i>S. decipiens</i> , <i>S. pachyantha</i> , <i>Sloanea</i> sp., <i>S. brevipes</i> , <i>S. echinocarpa</i> , <i>S. eichleri</i> , <i>S. garckeana</i> , <i>S. guianensis</i> , <i>S. latifolia</i> , <i>Stachyrrhena acuminata</i> , <i>Sterculia frondosa</i> , <i>S. liseae</i> , <i>S. multiflora</i> , <i>S. parviflora</i> , <i>Symphonia</i> sp., <i>S. globulifera</i> , <i>Symplocos martinicensis</i> , <i>Tachigali bracteolata</i> , <i>T. guianensis</i> , <i>T. melinonii</i> , <i>T. paniculata</i> , <i>T. paraensis</i> , <i>Talisia</i> sp., <i>T. clathrata</i> , <i>T. hexaphylla</i> , <i>T. microphylla</i> , <i>T. praeculta</i> , <i>T. simaboides</i> , <i>Tamarindus indica</i> , <i>Tapirira bethanniana</i> , <i>T. guianensis</i> , <i>T. obtusa</i> , <i>Tapura amazonica</i> , <i>T. capitulifera</i> , <i>T. guianensis</i> , <i>Tetragastris altissima</i> , <i>T. panamensis</i> , <i>Theobroma subincanum</i> , <i>T. velutinum</i> , <i>Thyrsodium guianense</i> , <i>T. puberulum</i> , <i>Torresea cearensis</i> , <i>Touroulia guianensis</i> , <i>Tomovita</i> sp., <i>Trachylobium hornemannianum</i> , <i>Trattinnickia</i> sp., <i>Trichilia cipo</i> , <i>T. euneira</i> , <i>T. micrantha</i> , <i>T. pallida</i> , <i>T. schomburgkii</i> , <i>T. surinamensis</i> , <i>Trymatococcus amazonicus</i> , <i>T. oligandrus</i> , <i>Unonopsis perrotteti</i> , <i>U. rufescens</i> , <i>Vatairea erythrocarpa</i> , <i>Vataireopsis surinamensis</i> , <i>Virola kwatae</i> , <i>V. michelii</i> , <i>V. multicostata</i> , <i>Vismia cayennensis</i> , <i>Vitex triflora</i> , <i>Vochysia guianensis</i> , <i>V. tomentosa</i> , <i>Vouacapoua americana</i> , <i>Vouararia guianensis</i> , <i>Xylopia nitida</i> , <i>Xylosma benthamii</i>
Other		<i>Acacia</i> sp., <i>A. auriculaeformis</i> , <i>Albertisia sessilis</i> , <i>Allophylus angustatus</i> , <i>A. latifolius</i> , <i>Betharocalyx salicifolius</i> , <i>Brosimum gaudichaudii</i> , <i>Buchanania arborescens</i> , <i>B. obovata</i> , <i>Byrsinima laxiflora</i> , <i>Callisthene major</i> , <i>Cassia alata</i> , <i>C. siamea</i> , <i>C. spruceana</i> , <i>Davilla elliptica</i> , <i>Denhamia obscura</i> , <i>Didymopanax macrocarpon</i> , <i>D. morototoni</i> , <i>Drypetes fanshawei</i> , <i>D. variabilis</i> , <i>Eremanthus glomerulatus</i> , <i>Erythroxylum daphnites</i> , <i>E. suberosum</i> , <i>Grevillea decurrens</i> , <i>Guapira areolata</i> , <i>G. graciliflora</i> , <i>Hymenaea courbaril</i> , <i>H. martiana</i> , <i>H. stigonocarpa</i> , <i>Inga laurina</i> , <i>Machaerium acuminata</i> , <i>M. opacum</i> , <i>Matayba guianensis</i> , <i>Maytenus floribunda</i> , <i>Miconia pohliana</i> , <i>Myrcia deflexa</i> , <i>M. rotundata</i> , <i>Myrseina guianensis</i> , <i>M. umbellatum</i> , <i>Ouratea castanæigolia</i> , <i>O. hexasperma</i> , <i>Piptocarpha macropoda</i> , <i>P. rotundifolia</i> , <i>Pouteria arnhemica</i> , <i>P. sericea</i> , <i>Pseudolmedia cf marginatum</i> , <i>Qualea dichotoma</i> , <i>Salacia crassifolia</i> , <i>Sophora chrysophylla</i> , <i>Styrax camporum</i> , <i>S. ferrugineus</i> , <i>Symplocos lanceolata</i> , <i>S. mosenii</i> , <i>Vochysia tucanorum</i>
TBD	RS	<i>Acosmium bijugum</i> , <i>Alphitonia excelsa</i> , <i>Brachystegia longifolia</i> , <i>B. spicaeformis</i> , <i>B. utilis</i> , <i>Burkea africana</i> , <i>Corymbia foelscheana</i> , <i>C. grandifolia</i> , <i>C. polycarpa</i> , <i>C. correcta</i> , <i>C. ptychocarpa</i> , <i>Gardenia resinosa</i> , <i>Isobertia paniculata</i> , <i>Petalostigma pubescens</i> , <i>Strychnos lucida</i> , <i>Swartzia arborescens</i> , <i>Tabebuia serratifolia</i> , <i>Terminalia carpentariae</i> , <i>T. ferdinandiana</i> , <i>T. latipes</i> , <i>Vitex glabrata</i>
NR		<i>Adenanthera macrocarpa</i> , <i>A. microsperma</i> , <i>A. pavonina</i> , <i>Adenocarpus viscosus</i> , <i>Aeschynomene elaphroxylon</i> , <i>A. pfundi</i> , <i>Affonseba bahiensis</i> , <i>Afzelia quanzensis</i> , <i>Andira anthelmia</i> , <i>A. fraxinifolia</i> , <i>A. inermis</i> , <i>A. laurifolia</i> , <i>A. nitida</i> , <i>A. paniculata</i> , <i>Antiaris toxicaria</i> , <i>Apelta glabra</i> , <i>A. petoumo</i> , <i>Aspidosperma discolor</i> , <i>Bauhinia candicans</i> , <i>B. purpurea</i> , <i>Bombacopsis nervosa</i> , <i>Bombaria</i> sp., <i>Butea frondosa</i> , <i>Byrsinima laevigata</i> , <i>Caesalpinia decapetala</i> , <i>C. myabensis</i> , <i>C. velutina</i> , <i>Caryocar glabrum</i> , <i>Cedrela</i> sp., <i>C. cateniformis</i> , <i>Chrysophyllum c. argenteum</i> , <i>C. cuneifolium</i> , <i>C. eximium</i> , <i>C. lucentifolium</i> , <i>C. prieurii</i> , <i>C. sanguinolentum</i> ,



**Table A1.** Continued.

PFT	Type	Species
TBD	NR	<i>Clitoria brachystegia</i> , <i>Copaifera trappezifolia</i> , <i>Cordia</i> sp., <i>C. sagotii</i> , <i>Couepia bracteosa</i> , <i>C. caryophylloides</i> , <i>C. guianensis</i> , <i>C. habrantha</i> , <i>C. joaquiniae</i> , <i>C. magnoliifolia</i> , <i>C. parillo</i> , <i>Couma guianensis</i> , <i>Cyathostegia mathewsi</i> , <i>Cylista scariosa</i> , <i>Delonix regia</i> , <i>Dialium guianense</i> , <i>Dimorphandra mollis</i> , <i>Dussia discolor</i> , <i>Eriotheca</i> sp., <i>E. longitubulosa</i> , <i>Erythrina aurantiaca</i> , <i>Erythrophleum guineense</i> , <i>E. lasianthum</i> , <i>Glycydendron amazonicum</i> , <i>Gouania glabra</i> , <i>Guettarda acreana</i> , <i>Himatanthus</i> sp., <i>Hirtella bicornis</i> , <i>H. bicornis</i> var <i>bicornis</i> , <i>H. bicornis</i> var <i>pubescens</i> , <i>H. glandistipula</i> , <i>H. glandulosa</i> , <i>H. macrosepala</i> , <i>H. suffulta</i> , <i>Hoffmannseggia intricata</i> , <i>Hymenolobium janeirens</i> , <i>Isernia</i> sp., <i>Jacaranda copaia</i> , <i>Laetia procera</i> , <i>Lecythis aurantiaca</i> , <i>Lonchocarpus capassa</i> , <i>L. floribundus</i> , <i>L. guatemalensis</i> , <i>L. leucanthus</i> , <i>Macrolobium bifolium</i> , <i>M. latifolium</i> , <i>M. palisotii</i> , <i>M. zenkeri</i> , <i>Matayba inlegans</i> , <i>M. laevigata</i> , <i>Milissa brahei</i> , <i>Mimosa caesalpiniifolia</i> , <i>M. scabrella</i> , <i>Myrospurum balsamiferum</i> , <i>M. frutescens</i> , <i>Ormosia nitida</i> , <i>Ostryocarpus riparius</i> , <i>Ouratea melinonii</i> , <i>Parapiptadenia pterosperma</i> , <i>Parinari campestris</i> , <i>P. excelsa</i> , <i>P. montana</i> , <i>Parkia velutina</i> , <i>Peltogyne</i> sp., <i>P. nitens</i> , <i>P. paniculata</i> , <i>Peltophorum africanum</i> , <i>P. pterocarpum</i> , <i>Phylloxylon perrieri</i> , <i>P. spinosa</i> , <i>Piptadenia buchananii</i> , <i>P. obliqua</i> , <i>P. viridiflora</i> , <i>Piscidia carthagagenensis</i> , <i>Pithecellobium selen</i> , <i>P. dulce</i> , <i>Platymiscium obtusifolium</i> , <i>P. pinnatum</i> , <i>P. zehnertii</i> , <i>Poepigia procera</i> , <i>P. prosera</i> , <i>Poinciana regia</i> , <i>Pongamia excoeca</i> , <i>P. pinnata</i> , <i>Pourouma melinonii</i> , <i>P. villosa</i> , <i>Pterocarpus angolensis</i> , <i>P. marsupium</i> , <i>P. osun</i> , <i>P. rhoiri</i> , <i>P. rotundifolius</i> , <i>P. santalinus</i> , <i>Pterodon abruptus</i> , <i>Pterogyne nitens</i> , <i>Rhynchosia clivorum</i> , <i>Sabinea carinalis</i> , <i>Schizolobium parahybum</i> , <i>Senna angustula</i> , <i>S. cana</i> , <i>Sterculia pruriens</i> , <i>S. speciosa</i> , <i>S. vilifera</i> , <i>Stryphnodendron moricicolor</i> , <i>S. polystachyum</i> , <i>Swartzia</i> sp., <i>S. acutifolia</i> , <i>S. amshoffiana</i> , <i>S. apetala</i> , <i>S. benthamiana</i> , <i>S. canescens</i> , <i>S. grandifolia</i> , <i>S. leblondii</i> , <i>S. oblanceolata</i> , <i>S. panacoco</i> , <i>S. panacoco</i> var. <i>panacoco</i> , <i>S. polyphylla</i> , <i>Tabebuia</i> sp., <i>T. capitata</i> , <i>Tarenna australis</i> , <i>Terminalia</i> sp., <i>T. guianensis</i> , <i>T. microcarpa</i> , <i>Tetrapleura ronnungii</i> , <i>Tipuana speciosa</i> , <i>Trattinnickia demerarae</i> , <i>Vantanea parviflora</i> , <i>Xylopia frutescens</i> , <i>Zygia racemosa</i> , <i>Z. tetragona</i>
Other		<i>Acacia kamerunensis</i> , <i>A. pennata</i> , <i>A. picachensis</i> , <i>A. tucumanensis</i> , <i>A. velutina</i> , <i>A. welwitschii</i> , <i>Aegiphila lhotskiana</i> , <i>A. sellowiana</i> , <i>Albizia adianthifolia</i> , <i>A. adinopephala</i> , <i>A. antunesiana</i> , <i>A. caribaea</i> , <i>A. forbesii</i> , <i>A. guachapele</i> , <i>A. petersiana</i> , <i>A. purpusii</i> , <i>A. sinaloensis</i> , <i>A. thompsoni</i> , <i>A. tomentosa</i> , <i>A. benthamiana</i> , <i>Aspidosperma subiricanum</i> , <i>A. tormentosum</i> , <i>Astrocarium rodrieguesii</i> , <i>A. sciophilum</i> , <i>Bauhinia cunninghamii</i> , <i>B. forficata</i> , <i>Blepharocarya depauperata</i> , <i>Brachychiton diversifolius</i> , <i>Byrsinoma crassa</i> , <i>Canarium australianum</i> , <i>Capparis leprieurii</i> , <i>C. maroniensis</i> , <i>Caryocar brasiliense</i> , <i>Cassia afrofistula</i> , <i>C. emarginata</i> , <i>C. fistula</i> , <i>C. laevigata</i> , <i>C. tomentosa</i> , <i>Centrobolium tomentosum</i> , <i>Dalbergia miscolobium</i> , <i>Eriotheca pubescens</i> , <i>Erythrophleum chlorostachys</i> , <i>Guapira noxia</i> , <i>Guettarda viburnoides</i> , <i>Hymenolobium</i> sp., <i>Hymenolobium flavum</i> , <i>Leucaena shannonii</i> , <i>Owenia vernicosa</i> , <i>Platypodium elegans</i> , <i>Pouteria ramiflora</i> , <i>Qualea parviflora</i> , <i>Tabebuia impetiginosa</i> , <i>T. ochracea</i> , <i>T. roseo-alba</i>
T.tN	N/A	<i>Abies alba</i> , <i>A. balsamea</i> , <i>A. cephalonica</i> , <i>A. cilicica</i> , <i>A. concolor</i> , <i>A. delavayi</i> , <i>A. grandis</i> , <i>A. lasiocarpa</i> , <i>A. lowiana</i> , <i>A. nordmanniana</i> , <i>A. recurvata</i> , <i>A. religiosa</i> , <i>A. sibirica</i> , <i>A. veitchii</i> , <i>Actinostrobus pyramidalis</i> , <i>Agathis australis</i> , <i>Arthrotaxis cupressoides</i> , <i>Agathis philippinensis</i> , <i>Araucaria angustifolia</i> , <i>A. bidwillii</i> , <i>A. columnaris</i> , <i>A. excelsa</i> , <i>Calitris</i> sp., <i>Cupressus</i> sp., <i>C. integrifolia</i> , <i>C. macroleayana</i> , <i>C. preissii</i> , <i>Calocedrus decurrens</i> , <i>Cedrus atlantica</i> , <i>C. deodara</i> , <i>Chamaecyparis lawsoniana</i> , <i>C. pisifera</i> , <i>Cryptomeria japonica</i> , <i>Cupressus arizonica</i> , <i>C. goveniana</i> , <i>C. guadalupensis</i> , <i>Dacrycarpus dacryodes</i> , <i>Dacrydium cupressinum</i> , <i>D. excelsum</i> , <i>Fitzroya cupressoides</i> , <i>Fokienia hodginsii</i> , <i>Glyptostrobus lineatus</i> , <i>Juniperus californica</i> , <i>J. cedrus</i> , <i>J. communis</i> , <i>J. deppeana</i> , <i>J. monosperma</i> , <i>J. occidentalis</i> , <i>J. osteosperma</i> , <i>J. J. oxycedrus</i> , <i>J. scopulorum</i> , <i>Picea</i> sp., <i>P. engelmannii</i> , <i>P. glauca</i> , <i>P. mariana</i> , <i>Pinus aristata</i> , <i>P. bahamensis</i> , <i>P. banksiana</i> , <i>P. canariensis</i> , <i>P. caribaea</i> , <i>P. coulteri</i> , <i>P. edulis</i> , <i>P. flexilis</i> , <i>P. halepensis</i> , <i>P. iopis</i> , <i>P. muricata</i> , <i>P. nigra</i> , <i>P. palustris</i> , <i>P. pinea</i> , <i>P. ponderosa</i> , <i>P. pungens</i> , <i>P. radiata</i> , <i>P. rigida</i> , <i>P. strobliformis</i> , <i>P. strobus</i> , <i>P. tabuliformis</i> , <i>P. taeda</i> , <i>Podocarpus</i> sp., <i>P. blumei</i> , <i>P. falcata</i> , <i>P. falcata</i> , <i>P. ferruginea</i> , <i>P. junghuhniana</i> , <i>P. latifolius</i> , <i>P. macrophylla</i> , <i>P. milanjiana</i> , <i>P. milanjianus</i> , <i>P. nagi</i> , <i>P. salignus</i> , <i>P. spicata</i> , <i>P. totara</i> , <i>P. transiens</i> , <i>Prumnopitys ferruginea</i> , <i>P. taxifolia</i> , <i>Pseudolarix amabilis</i> , <i>Pseudotsuga menziesii</i> , <i>Saxegothaea conspicua</i> , <i>Sciadopitys verticillata</i> , <i>Sequoioideae</i> , <i>Sequoiadendron giganteum</i> , <i>Serruria glomerata</i> , <i>Taxodium distichum</i> , <i>Taxus baccata</i> , <i>T. brevifolia</i> , <i>Thuja occidentalis</i> , <i>T. orientalis</i> , <i>T. plicata</i> , <i>T. standishii</i>

# Parameterisation of fire in LPX1 vegetation model

D. I. Kelley et al.

Title Page

## Abstract

Introduction

## Conclusions

## References

## Tables

## Figures



Back

Close

Full Screen / Esc

[Printer-friendly Version](#)

## Interactive Discussion



**Table A1.** Continued.

PFT	Type	Species
tBE	RS	<i>Acacia karroo, A. luederitzii, Corymbia gummifera, Elaeocarpus reticulatus, E. amygdalina, E. bridgesiana, E. prava, E. saligna, E. botryoides, E. cameronii, E. nobilis, Leucospermum conocarpodendron, Mimetes fimbriifolius, Orites excelsa, Protea nitida, Ulex europaeus, Vesselowskyia rubriflora</i>
	NR	<i>Acacia sp., A. baileyana, A. decurrens, A. maidenii, A. verticillata, A. maidenii, Ammodendron karelinii, Androstachys johnsonii, Anopterus glandulosus, Aristotelia serrata, Ateleia tomentosa, Aulax umbellata, Banksia integrifolia ssp. monticola, Bauhinia galpinii, Beilschmiedia tawa, Cadia ellisiaana, Caesalpinia arenosa, C. cacalaco, C. caladenia, C. californica, C. epiphanoia, C. eriostachys, C. exostemma, C. gaumeri, C. glabrata, C. gracilis, C. hilderbrandtii, C. hintonii, C. hughesii, C. madagascariensis, C. melanadenia, C. mexicana, C. nipensis, C. palmeri, C. pannosa, C. placida, C. standleyi, C. violacea, C. yucatanensis, Callistachys lanceolata, Carpodetus serratus, Chamaesyctis palmensis, C. prolifera, Chlorocalyx confine, Cordeauxia edulis, Cytisus battandieri, Dalbergia hupeana, Dendrocnide excelsa, Elaeodendron transvaalense, Eucalyptus regnans, Eucalyptus cf. marginata, Gymnocladus dioica, Harpalice arborescens, Hebestigma cubense, Hoheria cf. sexstylosa, Hybosoma ehrenbergii, Laurelia novae-zelandiae, Leucadendron argenteum, L. lauraeolum, L. xanthoconus, Lnochocarpus acuminatus, Naucleopsis guianensis, Neea sp., Pickeringia montana, Plinia rivularis, Podocarpus elatus, Poralyria cyathula, Prosopis glandulosa, Prostanthera sp. aff. lasianthos, Protea coronata, P. lepidocarpodendron, P. repens, P. roupelliae, Pseudopanax arboreus, P. crassifolius, Raukaua edgerleyi, Sassafras albidum, Schotia brachypetala, S. capitata, Spartocytisus nubigenus, S. supranubius, Sterculia quadrifida, Styx pallidus, Syzygium maire, Warburgia salutaris, Weinmannia racemosa, Xanthocercis zambesiaca</i>
Other		<i>Acacia brandegeana, A. choriophylla, A. coulteri, A. dealbata, A. eburnea, A. ehrenbergiana, A. farnesiana, A. floribunda, A. huarango, A. laeta, A. longifolia, A. macracantha, A. mammifera, A. melanoxyylon, A. mellifera, A. nerifolia, A. nubica, A. pataczekii, A. pennivenia, A. pterygota, A. raddiana, A. senegal, A. seyal, A. sieberana, A. sowdenii, A. spirocarpa, A. swazica, A. willardiana, Acmena smithii, A. smithii, Atherosperma moschatum, Aulax pallasia, Calodruvia paniculata, Callicoma seratifolia, Calycotome villosa, Cassia montana, C. polyantha, C. pringlei, C. skinneri, Cerratopetalum apetaum, Cordyline australis, Cryptocaria nova-anglica, C. meissneriana, Doryphora sassafrass ssp montane, Elaeocarpus holopetalus, E. dentatus, E. australis, Endiandra sieberi, Eucalyptus coccifera, E. obliqua, E. rubida, E. pauciflora, Eucryphia lucida, Glischodon ferdinandii, Guioa semiglaucia, Hedycarya arborea, Indigofera marmorata, I. oblongifolia, I. teysmanni, Kunzea ericoides, Leucadendron salignum, Leucaena diversifolia, Lophostemon confertus, Mimetes cucullatus, Nothofagus cunninghamii, N. moorei, Notelaea sp. aff. venosa, Phyllocladus aspleniifolius, Pittosporum undulatum, Pomaderis apetala, Pomaderis apetala, Protea caffra, P. cynaroides, Quintinia sieberi, Rapanea variabilis, Schizomeria ovata, Sophora affinis, S. microphylla, S. tetrapeta, S. tomentosa, Tasmania stipitata, Trichilia emetica, Trochocarpa montana</i>
tBD	RS	<i>Acacia gerrardii, A. grandicornuta, A. nigrescens, A. tortilis, Acer glabrum, A. grandidentatum, Betula papyrifera, Brachystegia boehmii, Cercis siliquastrum, Colophospermum mopane, Corymbia polystyota, Genista acanthoclada, Populus angustifolia, P. balsamifera, P. tremuloides, Sclerocarya birrea, Toona ciliata, Ziziphus mucronata</i>
	NR	<i>Acacia xanthophloea, Acer negundo, Alnus oblongifolia, Apoplanesia paniculata, Balanites maughamii, Bauhinia roxburghiana, B. subrotundifolia, Brya ebenus, Caesalpinia platyloba, C. sclerocarpa, Calliandra houstoniana, Carmichaelia australis, Cercidium floridum ssp. peninsulare, C. microphyllum, C. peninsulare, C. praecox, C. texanum, Colvillea racemosa, Conzattia multiflora, Coursetia glandulosa, Cyrtisus candicans, C. proliferus, Dalbergia melanoxyylon, Desmanthus fruticosus, Desmodium tiliaeefolium, Diphysa americana, Elephantorrhiza burkei, Enterolobium contortisiliquum, Enterolobium cyclocarpum, Eysenhardtia amorphoides, Fordia cf. brachybotrys, Fraxinus velutina, Fuchsia excorticata, Genista benehoavensis, G. cinerea, G. virgata, Geoffroea decorticans, Goodia lotifolia, Gymnocladus canadensis, Juglans major, Kirkia acuminata, Lemuripusum edule, Lysiloma aurita, L. candida, Mimosa benthamii, Mimosia falcatula, Olneya tesota, Peleophorum dubium, Phyllocarpus septentrionalis, Piscidia mollis, P. pispilla, Pithecellobium glaucum, P. unguis-cati, Platanus wrightii, Populus fremontii, Prunus emarginata, Retama monosperma, Rhus chirindensis, R. glabra, Robinia x holtii britzensis, Salix sp., S. babylonica, S. bebbiana, Sesbania sesban, Spartium junceum, Teline stenopetala</i>

Title Page

Abstract

Introduction

Conclusions

References

Tables

Figures



Back

Close

Full Screen / Esc

Printer-friendly Version

Interactive Discussion

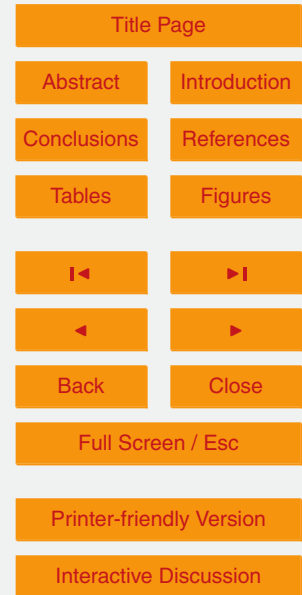


## Parameterisation of fire in LPX1 vegetation model

D. I. Kelley et al.

**Table A1.** Continued.

PFT	Type	Species
tBD	Other	<i>Acacia albida, A. angustissima, A. caffra, A. chameleensis, A. davyi, A. exuvialis, A. horrida, A. nilotica, A. robusta, Albizia anthelmintica, A. occidentalis, A. plurijuga, A. versicolor, Calycotome spinosa, Cassia abbreviata, C. wislizenii, Celtis reticulata, Combretum hereroense, C. imberbe, Cyrtus scorpiarius, Dichrostachys cinerea, Gleditsia triacanthos, Laburnum anagyroides, Leucaena confertiflora, L. esculenta, L. esculenta x leucocephala, L. macrophylla, L. pulverulenta, Quercus gambelii, Robinia neomexicana, R. pseudoacacia, Sophora japonica, S. secundiflora, Terminalia prunioides, T. sericea</i>
BN	N/A	<i>Picea abies, P. jezoensis, P. likiangensis, P. obovata, P. omorica, P. orientalis, P. purgans, P. schrenkiana, P. spinulosa, Pinus cembra, P. cembroides, P. gerardiana, P. koraiensis, P. laticio, P. longifolia, Tsuga canadensis, T. dumosa, T. heterophylla</i>



# Parameterisation of fire in LPX1 vegetation model

D. I. Kelley et al.

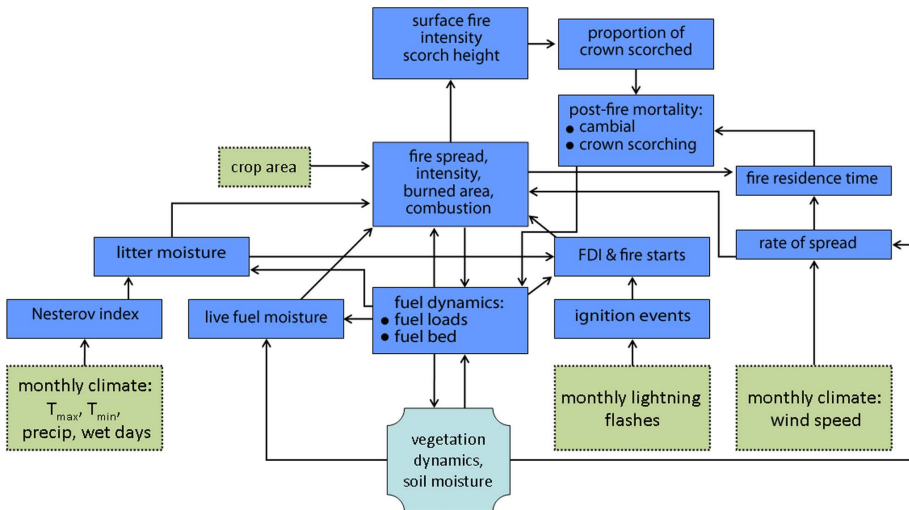


**Fig. 1.** Description of the structure of the fire component of LPX, reproduced from Prentice et al. (2011). Inputs to the model are identified by green boxes, outputs from the vegetation dynamics component of the model are identified by light blue boxes, and internal processes and exchanges that are explicitly simulated by the fire component of the model are identified by blue boxes.

991

**Fig. 2.** Observed relationships between (a) total and cloud-to-ground lightning flashes, (b) the percentage of dry lightning with respect to the number of wet days per month, and (c) percentage of dry days with lightning with respect to monthly dry lightning strikes. These analyses are based on the Lightning Image Sensor (LIS) remote sensed data set (Christian et al., 1999; Christian, 1999) and NLDN ground observation of lightning strikes (Cummins and Murphy, 2009) for North America. The red line shows best-fit used by LPX-Mv1, the red dotted line shows the mean of the observations, and the blue line shows the relationship used in LPX. To aid visualisation, observations were binned every 1 % (b) or 0.1 strikes (c) along the x-axis, with the dots showing the mean of each bin and the error bars showing the standard deviations.

Parameterisation of  
fire in LPX1  
vegetation model

D. I. Kelley et al.

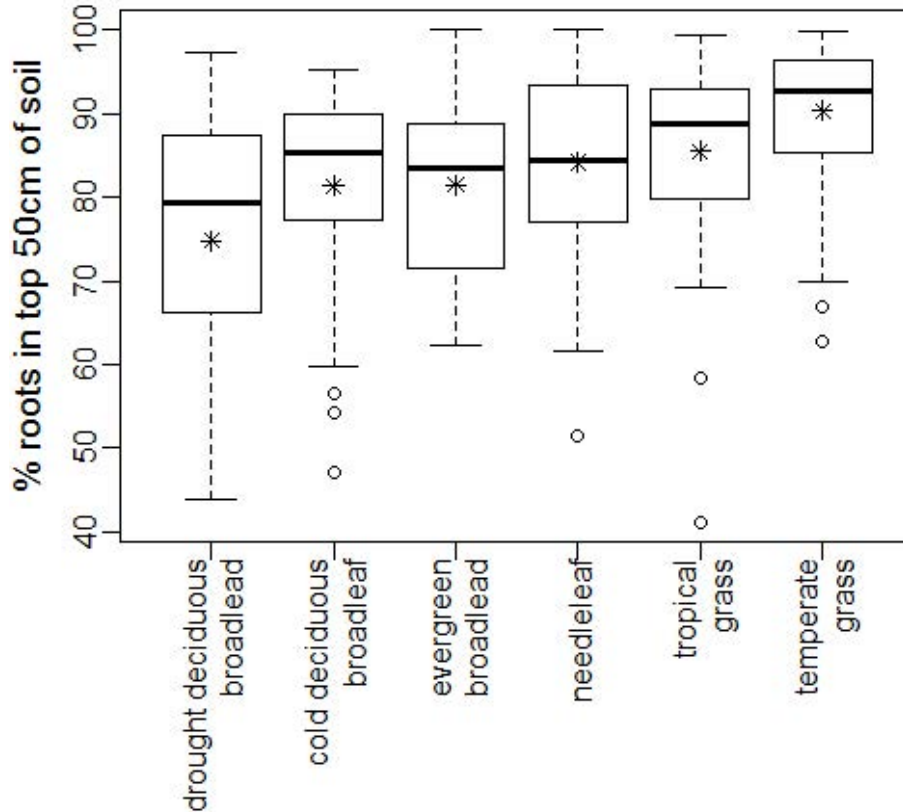
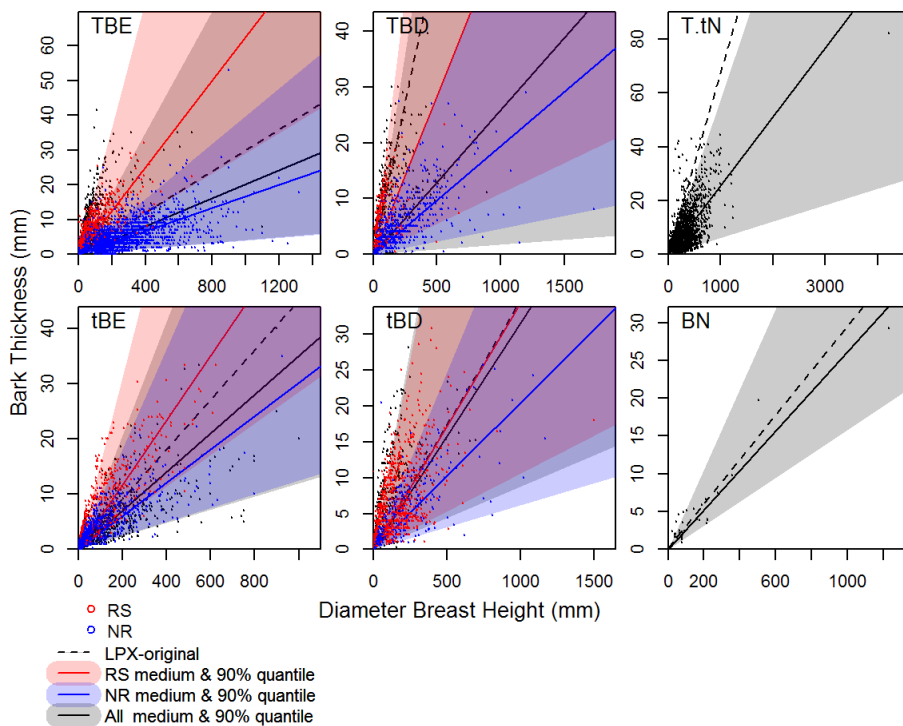


**Fig. 3.** Proportion of roots in the upper 50 cm of the soil by Plant Functional Type (PFT). The data were derived from Schenk and Jackson (2002a, 2005) and reclassified into the PFT recognized by LPX as shown in Table 2.

## Parameterisation of fire in LPX1 vegetation model

D. I. Kelley et al.



## Parameterisation of fire in LPX1 vegetation model

D. I. Kelley et al.

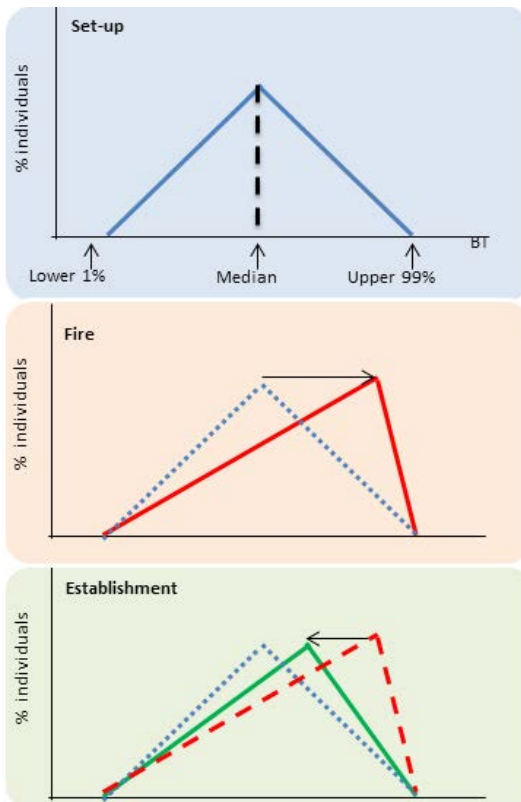


**Fig. 5.** Illustration of the variable bark thickness scheme. The initial set-up is based on parameter values (Table 1) obtained from Fig. 4. Fire preferentially kills individual plants with thin bark, changing the distribution towards individuals with thicker bar. Establishment shifts the distribution back towards the initial set-up.

## Parameterisation of fire in LPX1 vegetation model

D. I. Kelley et al.

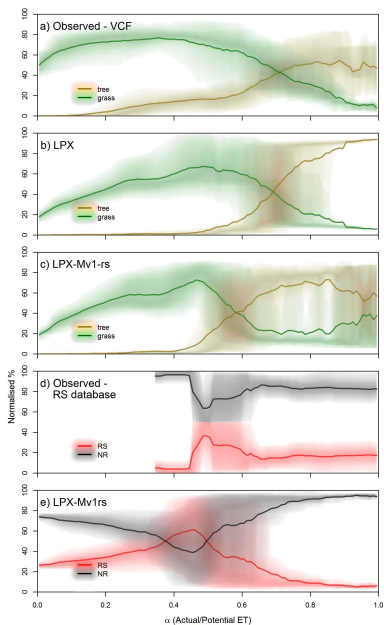


**Fig. 6.** Comparison of the simulated abundance of grass, tree and resprouting trees along the climatic gradient in moisture, as measured by  $\alpha$  (actual: potential evapotranspiration). Remotely sensed observations (**a**) of tree and grass cover from (DeFries and Hansen, 2009) compared to distribution of grass and trees simulated (**b**) by LPX and (**c**) LPX-Mv1-rs. (**d**) Observations of the abundance of aerial resprouters (RS – red) and other species (NR – black) from Harrison et al. (2014) compared to (**e**) RS (red) and non-resprouting (NR) PFTs (black) simulated by LPX-Mv1-rs. Note that some of the species included in the observed NR category may exhibit post-fire recovery behaviours such as underground (clonal) regrowth.  $\alpha$  was calculated as described by Gallego-Sala et al. (2010) in (**a**) and (**d**); and simulated by the relevant model in (**b**), (**c**) and (**e**). Abundance in (**d**) and (**e**) is normalised to show the % of the total vegetative cover of each category. Solid lines denote the 0.1 running mean and shading denotes the density of sites based on quantiles for each 0.1 running interval of  $\alpha$ .

# Parameterisation of fire in LPX1 vegetation model

D. I. Kelley et al.

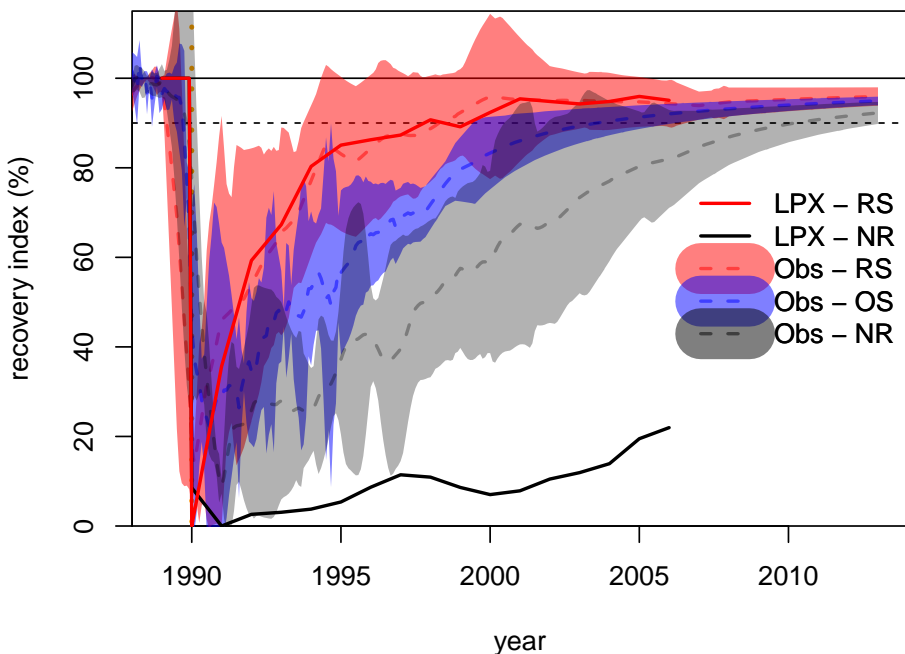


**Fig. 7.** Simulated time to recovery after fire compared to observed time to recovery. Red denotes ecosystems dominated by above-ground resprouting (RS) species; blue denotes other fire-adapted species, mostly obligate seeders (OS); black denotes vegetation which does not display specific fire adaptations (NR). The solid lines show LPX simulations; dotted lines show the mean of the relevant observations; the shaded areas show interquartile ranges of the relevant observations.

Title Page

Abstra

## Introduction

## Conclusion

## References

Table:

## Figures



Back

Close

Full Screen / Esc

[Printer-friendly Version](#)

## Interactive Discussion



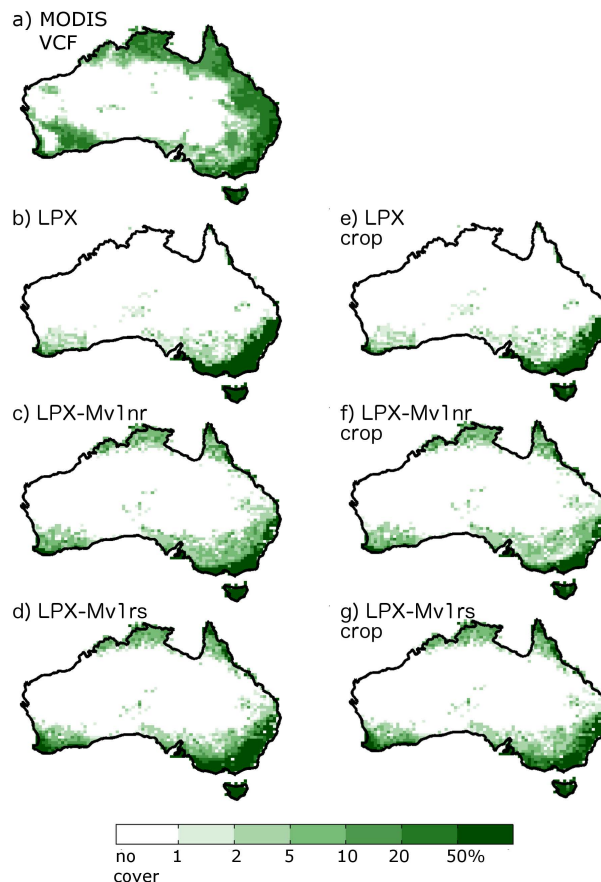


**Fig. 8.** Comparison of % tree cover from (a) observations (DeFries and Hansen, 2009) and as simulated by LPX-M, LPX-Mv1-nr and LPX-Mv1-rs without (b–d respectively) and with (e–g respectively) crop masking.

**Parameterisation of fire in LPX1 vegetation model**

D. I. Kelley et al.

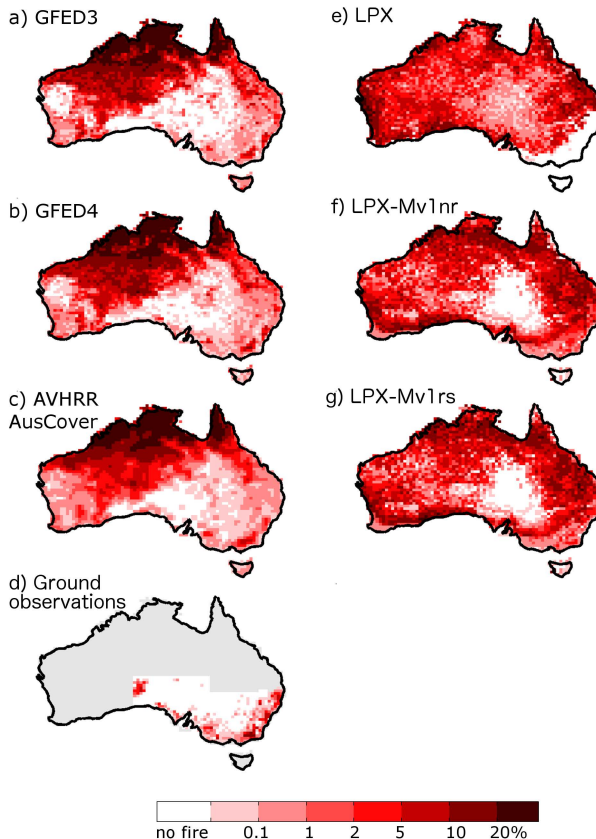


**Fig. 9.** Annual average burnt area between 1997–2005 based on observations from (a) Global Fire Database version 3 (GFED3: Giglio et al., 2010); and (b) version 4 (GFED4: Giglio et al., 2013); (c) Advanced Very High Resolution Radiometer (AVHRR: Maier and Russell-Smith, 2012); (d) southeastern Australia ground observations (Bradstock et al., 2013); and as simulated by (e) LPX; (f) LPX-Mv1-nr; (g) LPX-Mv1-rs.

**Parameterisation of fire in LPX1 vegetation model**

D. I. Kelley et al.

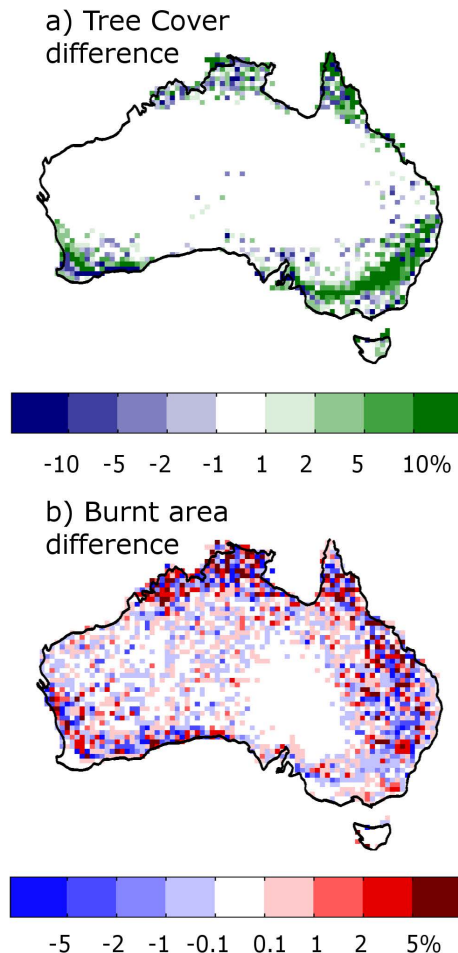


**Fig. 10.** The difference in (a) tree cover and (b) burnt area between the non-resprouting (LPX-MV1-nr) and resprouting (LPX-Mv1-rs) versions of LPX.